3D Spatial Imaging: from JLab 12 GeV to the EIC

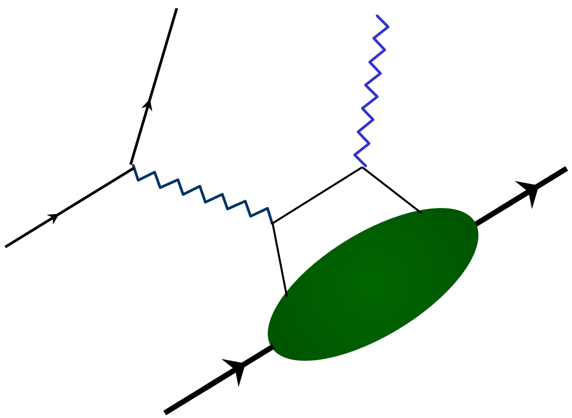

Daria Sokhan

University of Glasgow, Scotland

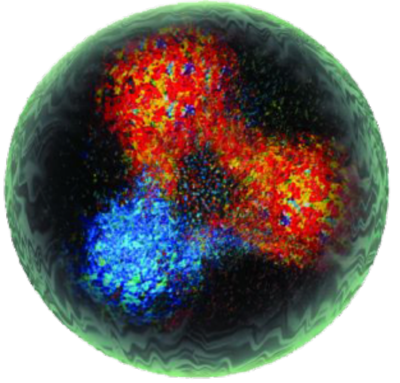

Lecture course for the 33rd annual Hampton University Graduate Studies Programme (HUGS)

29th May - 15th June 2018
Jefferson Lab, Virginia, USA

General outline of lecture material:

* Imaging at the sub-nucleon scale, Generalised Parton Distributions and how to access them
* Deeply Virtual Compton scattering
* Deeply Virtual Meson Production
* Experimental measurements @ JLab
* What we have learned pre JLab-12
* Tomography with JLab-12 and the EIC

(5 lectures)

An abridged history of nucleon imaging

Before 1956: the nucleon is point-like and fundamental…

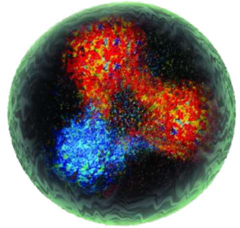

1960s: the Quark Model. Nucleons are composed of three valence quarks!
Gell-Mann (Nobel Prize 1969), Zweig.

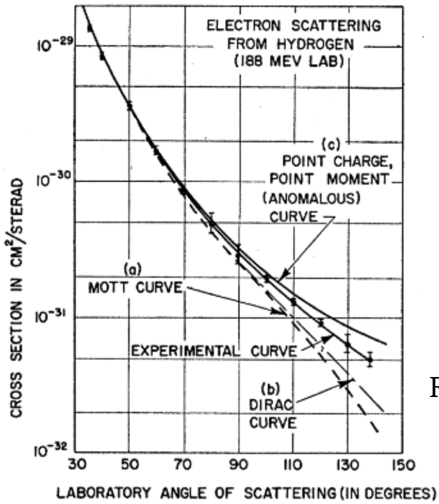

Robert Hofstadter
1915 - 1990
(Wikipedia)

1968: Deep Inelastic scattering at SLAC: scaling observed. The proton consists of point-like charges: partons!
Friedman, Kendall, Taylor: Nobel Prize 1990

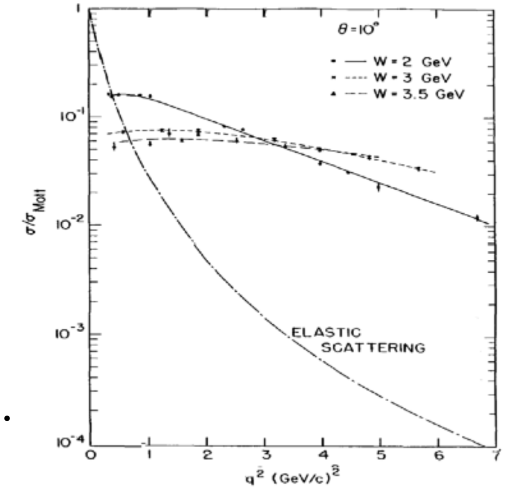

1972: Theory of QCD developed.

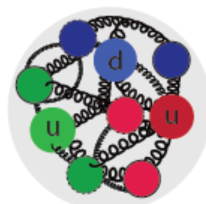

1956: Elastic scattering at SLAC: the proton has internal structure!
Hofstadter: Nobel Prize 1961.

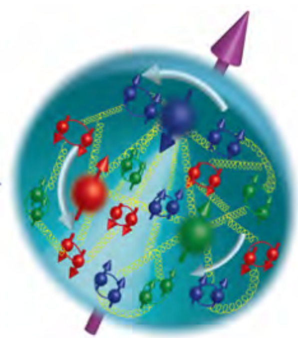

1970s-1990s: Deep Inelastic Scattering reveals a rich structure: quark-gluon sea, flavour distributions, puzzles of spin… what you see depends on how closely you look!

21st Century: High-precision imaging of quarks and gluons. 3D tomography of the nucleon: spatial and momentum distributions inside it across all scales.

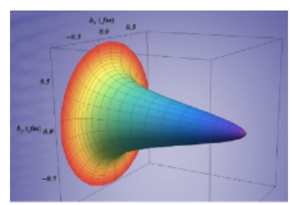

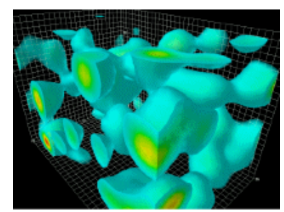

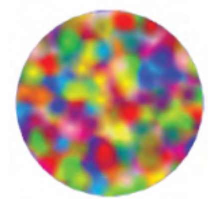

Electron scattering: a reminder of terminology

Elastic scattering: initial and final state is the same, only momenta change.

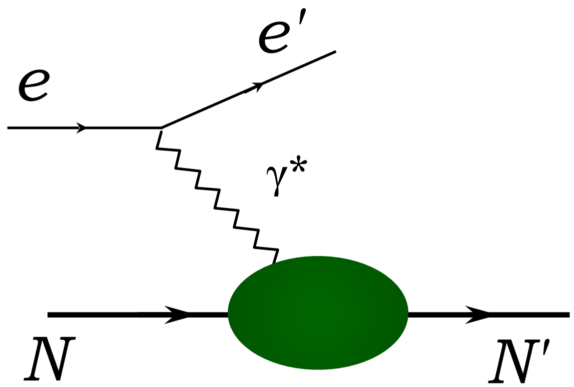

Deep inelastic scattering (DIS): state of the nucleon changed, new particles created.

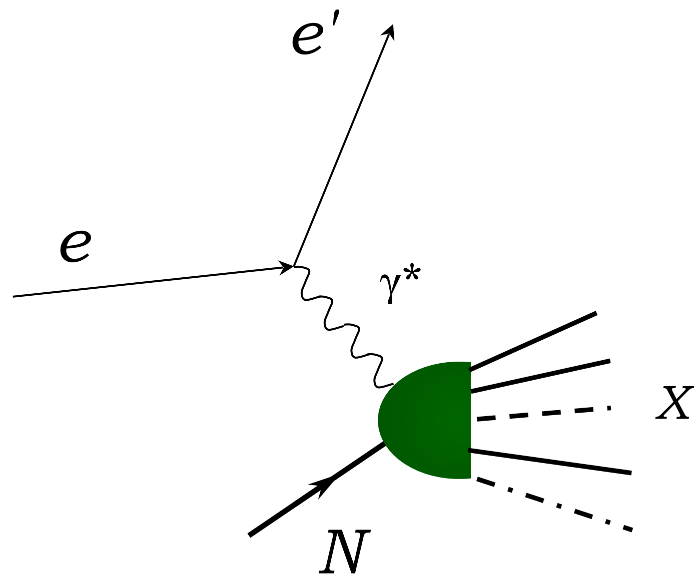

Measurements:

★ Inclusive — only the electron is detected
★ Semi-inclusive — electron and typically one hadron detected
★ Exclusive — all final state particles detected

→ Complementary information on the nucleon's structure

Scales of resolution – an elephantine analogy

Lyuba, baby mamoth found in Siberia, imaged with visible light…

International Mammoth Committee

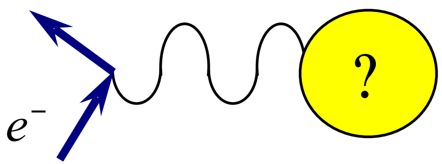

Q^2 ~ MeV^2

Scales of resolution – an elephantine analogy

Lyuba, baby mamoth found in Siberia, imaged with visible light…

… and X-rays.

International Mammoth Committee

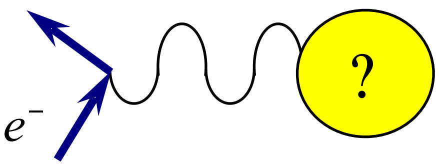

Q^2 ~ MeV^2

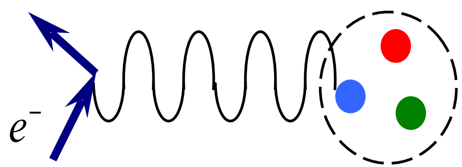

Q^2 >> GeV^2

Equivalent wavelength of the probe:

$$\lambda \approx \frac{1}{\sqrt{Q^2}}$$

What you see depends on what you use to look…

The 2D spatial image

Lepton (eg: electron, neutrino) scattering off a nucleon reveals different aspects of nucleon structure.

Elastic Scattering

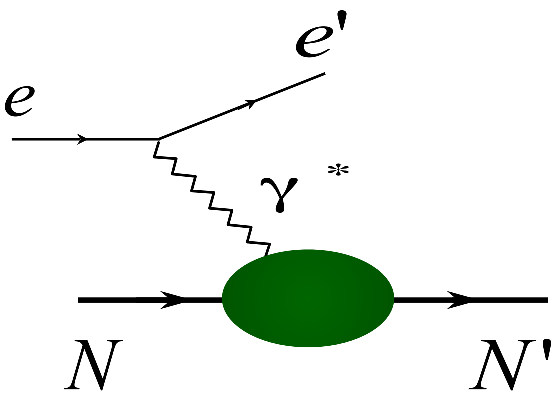

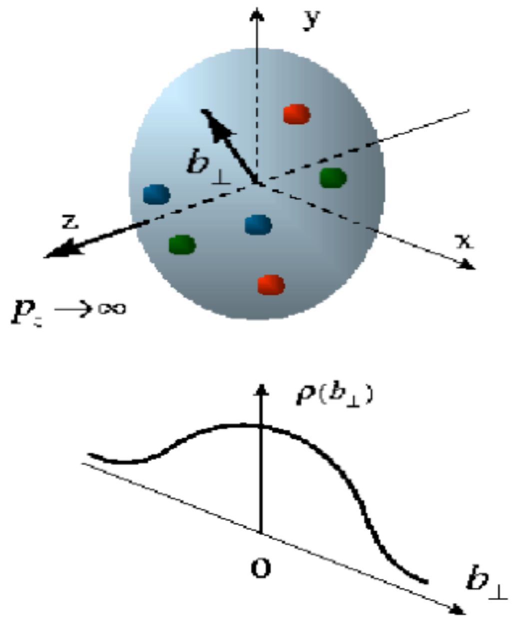

Cross-section parameterised in terms of Form Factors (Pauli, Dirac, axial, pseudo-scalar)

Transverse quark distributions: charge, magnetisation.

Charge density inside a nucleon

Proton

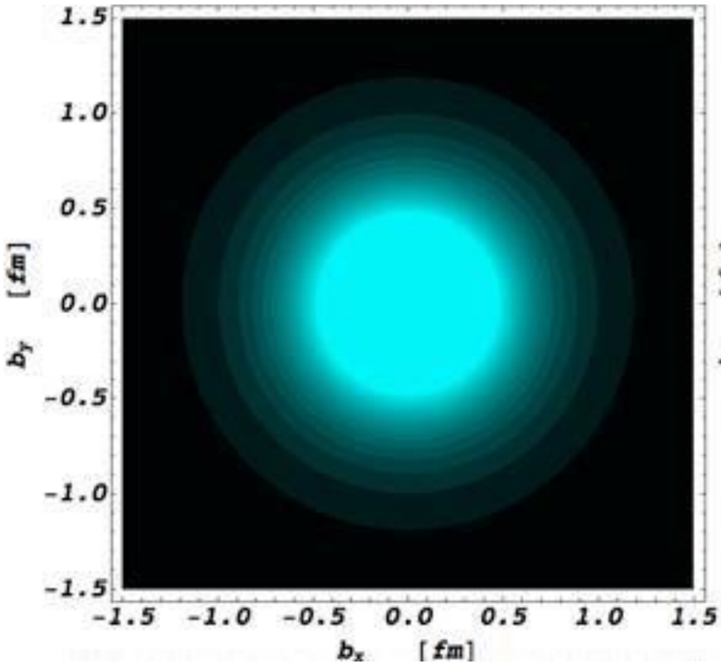

Neutron

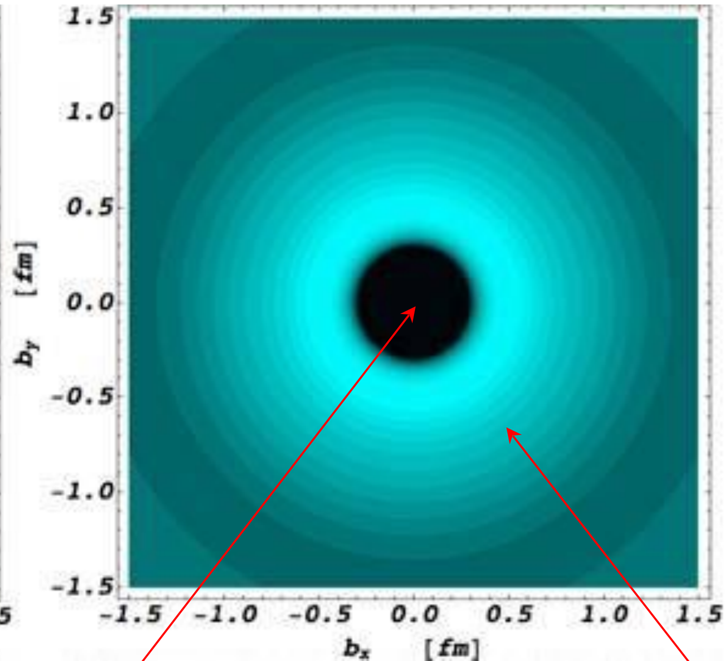

negative inner core

positive outer surface

C. Carlson, M. Vanderhaeghen
PRL 100, 032004 (2008)

A dynamical image

Deep Inelastic Scattering

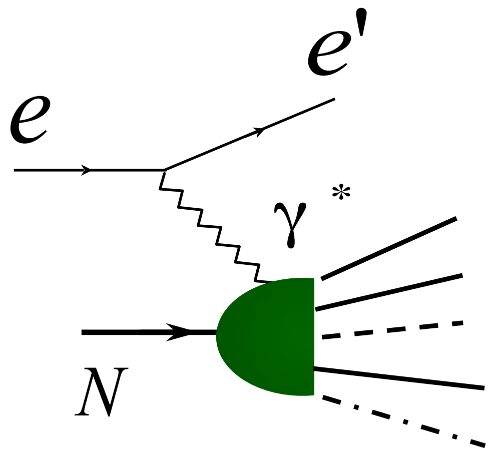

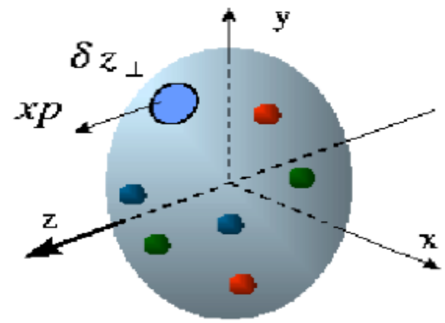

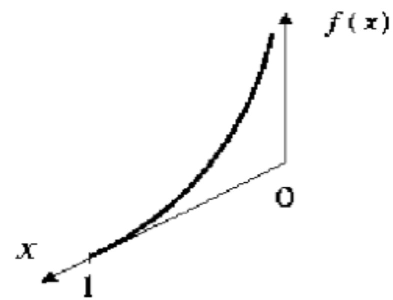

First experimental evidence of partons inside a nucleon

Cross-section parameterised in terms of polarised and unpolarised Structure Functions

→ Longitudinal momentum and helicity distributions of partons

Parton Distribution Functions

Momentum distributions of quarks and gluons within a nucleon.

x: longitudinal momentum of parton as a fraction of nucleon's momentum.

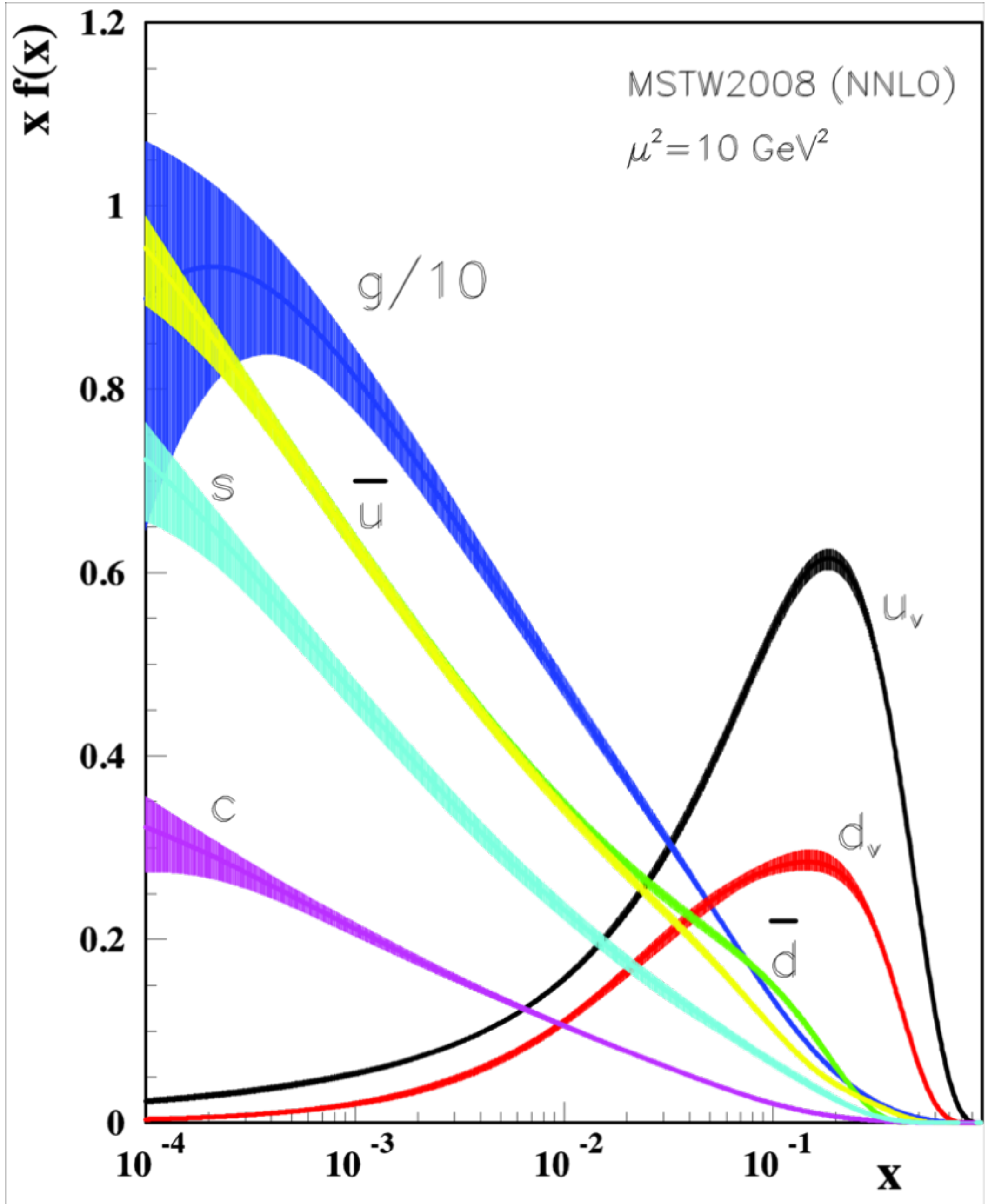

A full “knowledge” of the nucleon…

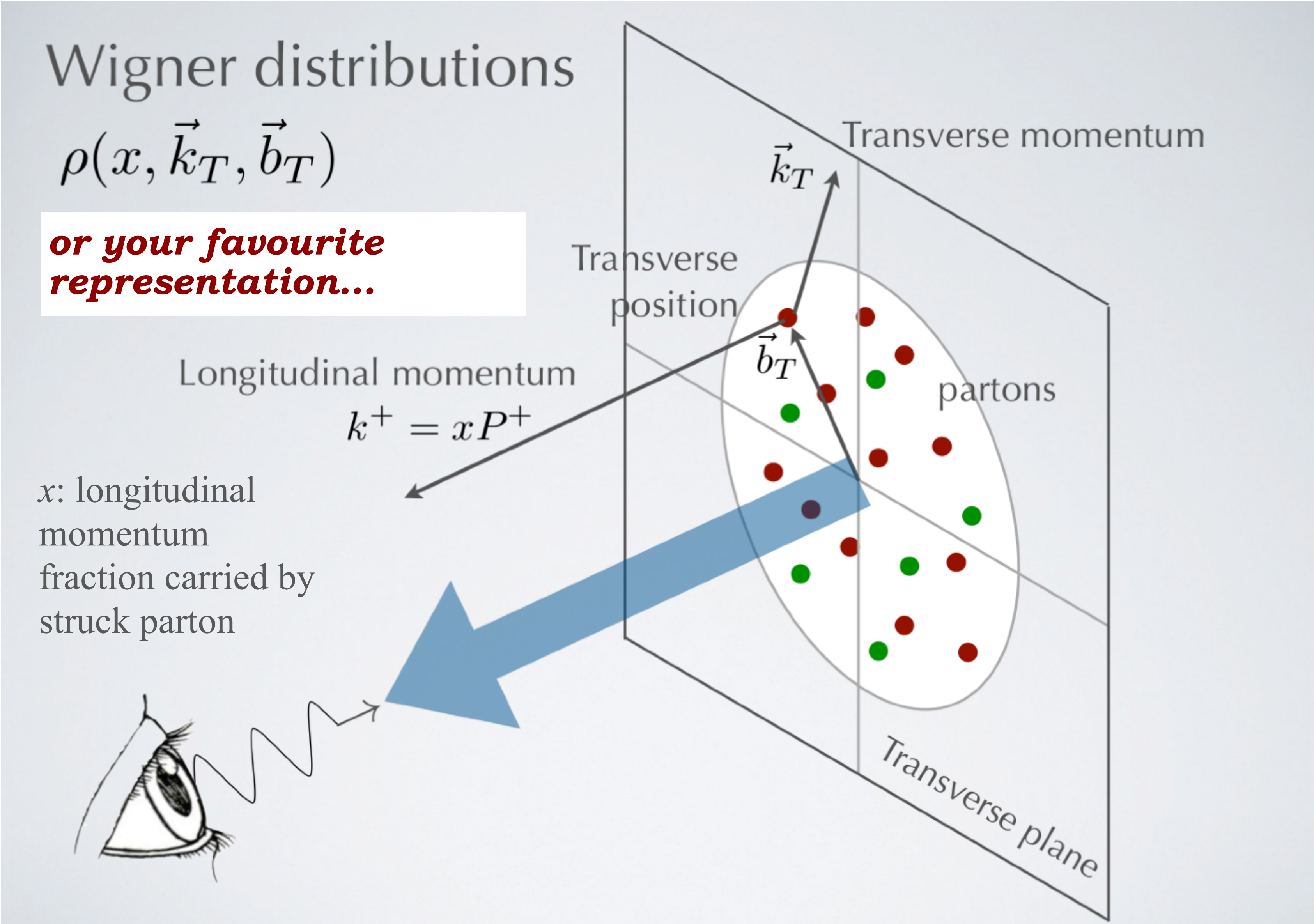

… is hard to come by

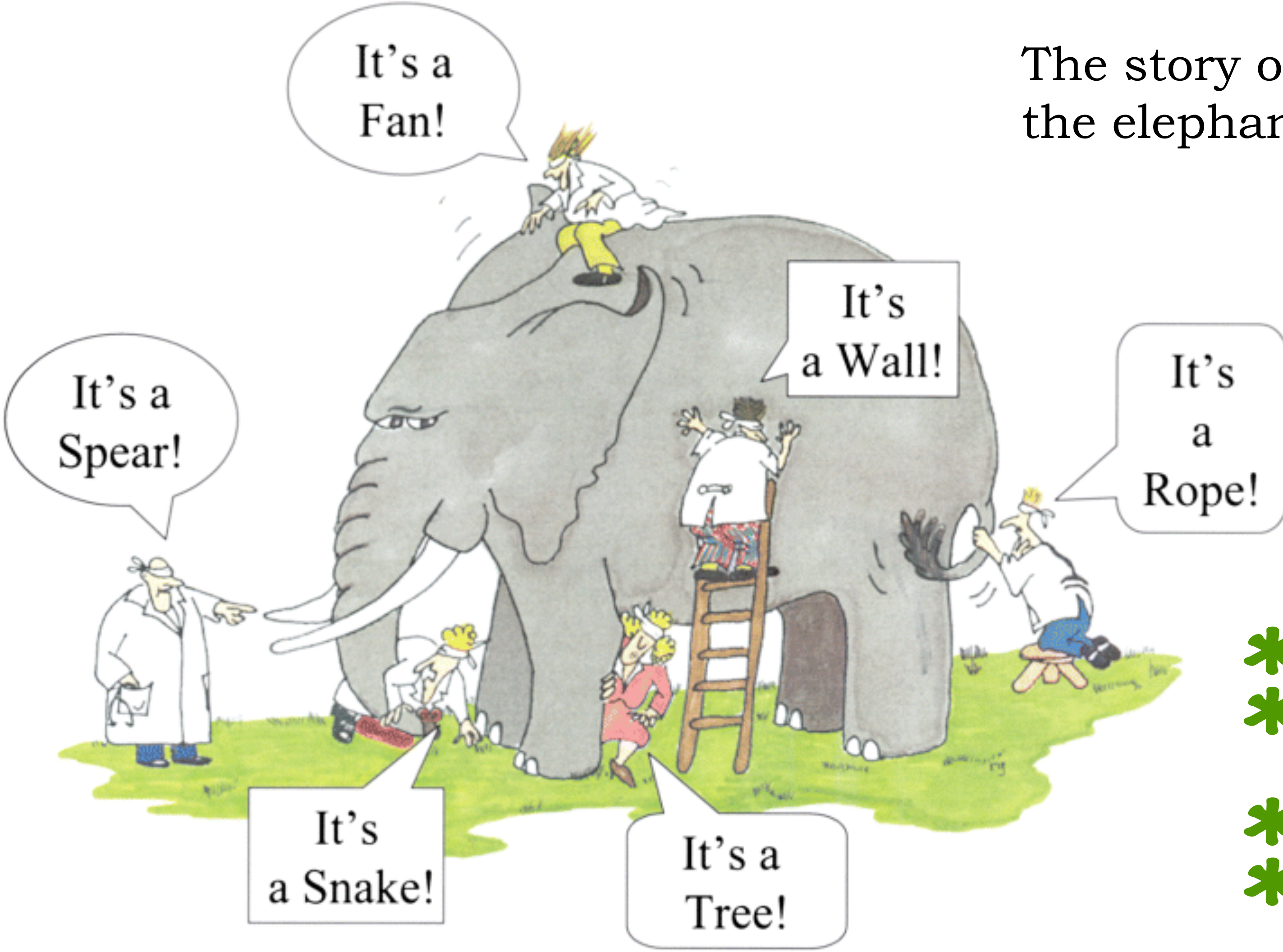

The story of the blind men and the elephant.

- Elastic scattering
- Deep Inealstic Scattering (DIS)
- Semi-inclusive DIS
- Deep exclusive reactions

G. Renee Guzlas, artist.

What you see depends also on how you look…

Images of the nucleon

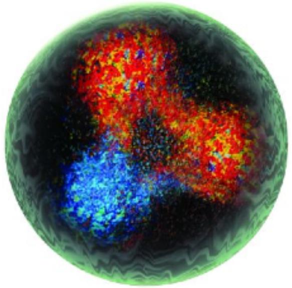

Wigner function:
full phase space parton
distribution of the nucleon

$\int d^2 b_T$

Transverse Momentum Distributions (TMDs)

* Semi-inclusive DIS

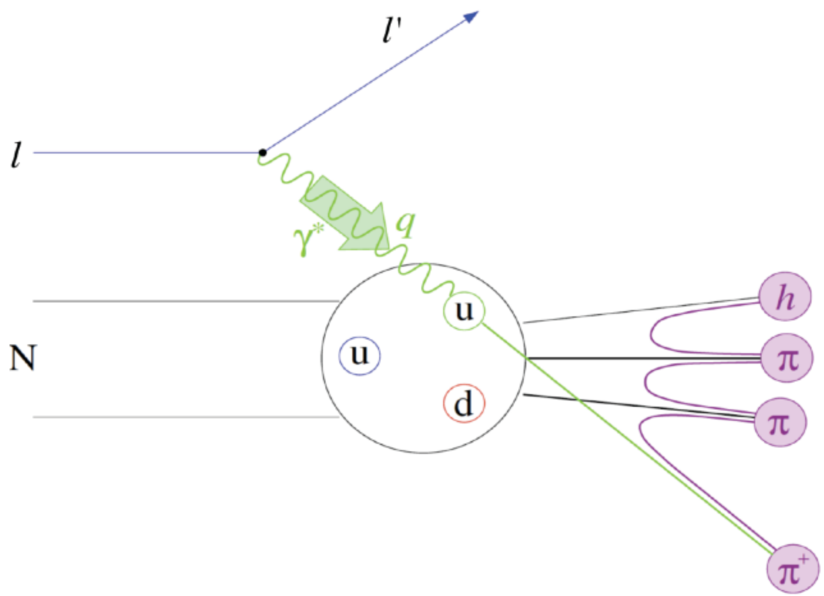

Images of the nucleon

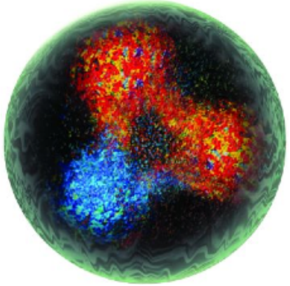

Wigner function:
full phase space parton distribution of the nucleon

$$\int d^2 b_T$$

Transverse Momentum Distributions (TMDs)

$$\int d^2 k_T$$

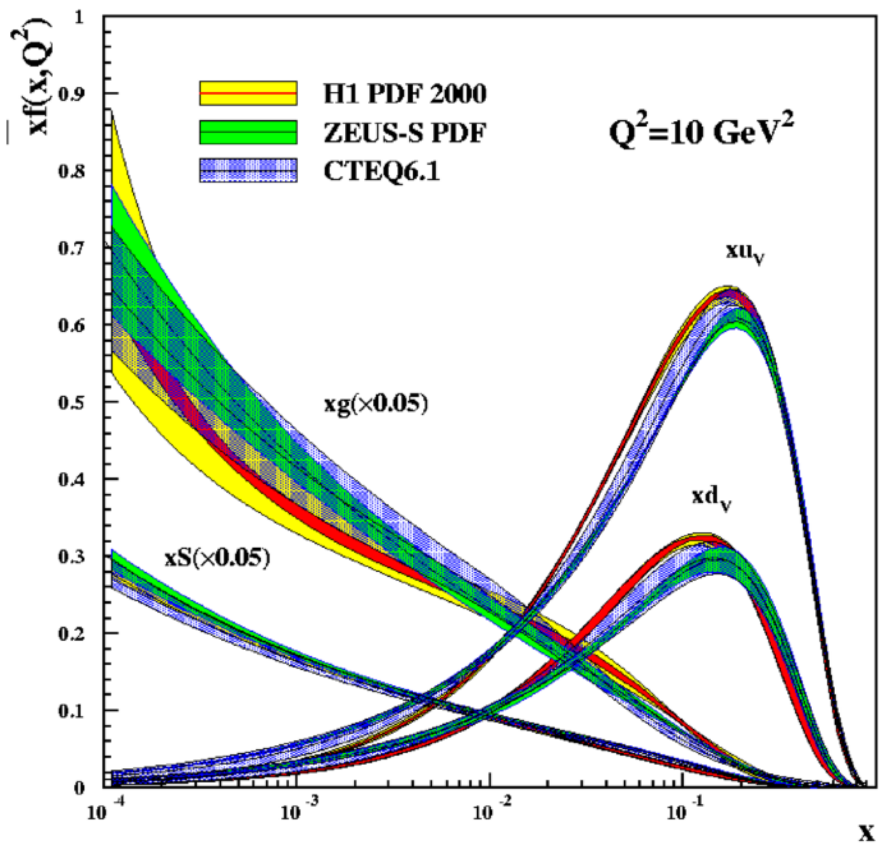

Parton Distribution Functions (PDFs)

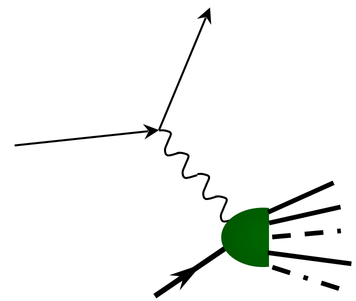

* Deep Inelastic Scattering

Images of the nucleon

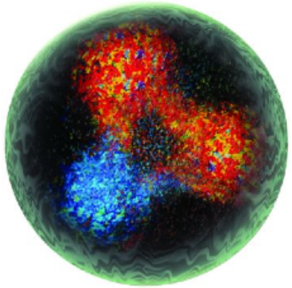

Wigner function:
full phase space parton distribution of the nucleon

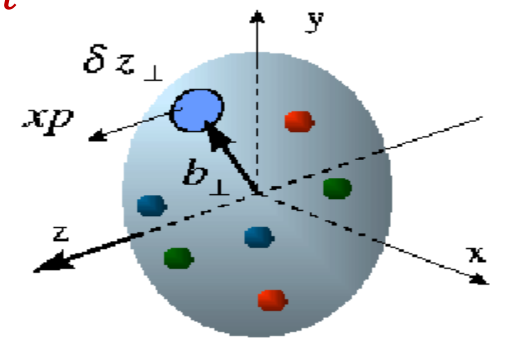

$$\int d^2 k_T$$

Generalised Parton Distributions (GPDs)

- relate, in the infinite momentum frame, transverse position of partons ($b_\perp$) to longitudinal momentum (x).

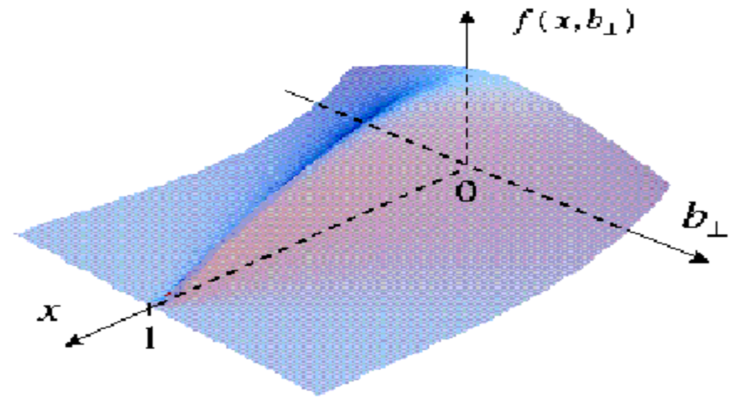

* Deep exclusive reactions, e.g.: Deeply Virtual Compton Scattering, Deeply Virtual Meson production, …

Images of the nucleon

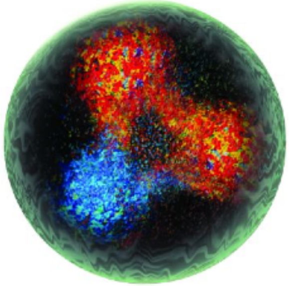

Wigner function:
full phase space parton distribution of the nucleon

$$\int d^2 k_T$$

Generalised Parton Distributions (GPDs)

$$\int dx$$

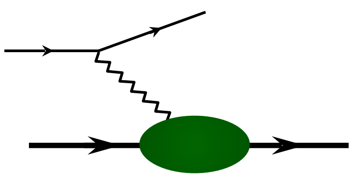

Form Factors
eg: $G_{E,}\, G_M$

Fourier Transform of electric Form Factor: transverse charge density of a nucleon

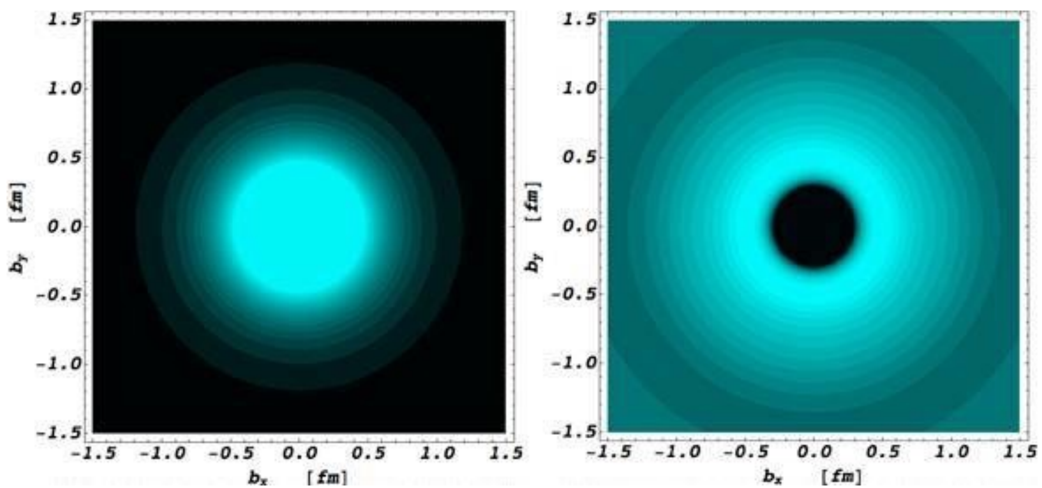

proton neutron

C. Carlson, M. Vanderhaeghen
PRL 100, 032004 (2008)

Images of the nucleon

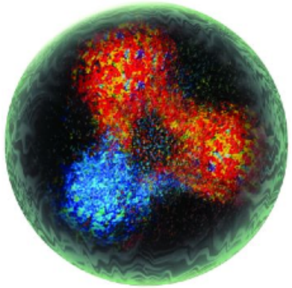

Wigner function:
full phase space parton
distribution of the nucleon

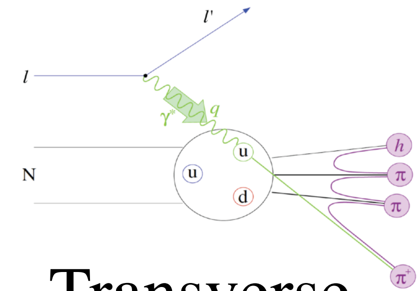

$\int d^2k_T$

$\int d^2b_T$

Generalised Parton Distributions (GPDs)

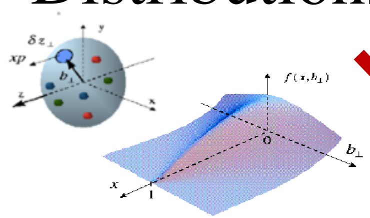

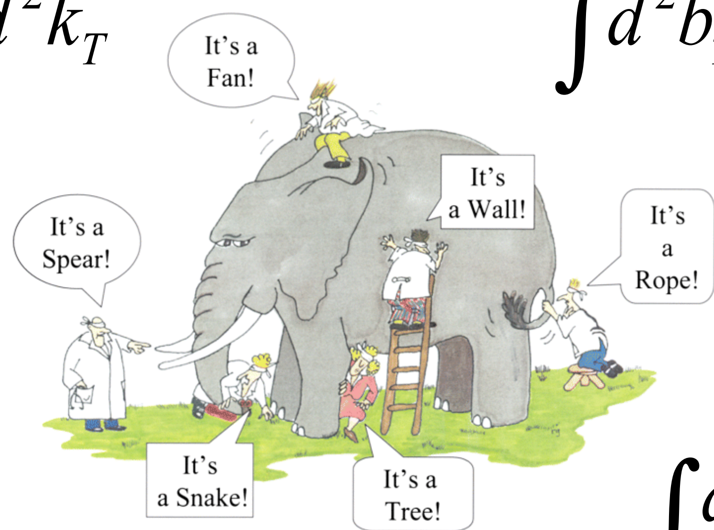

G. Renee Guzlas, artist.

Transverse Momentum Distributions (TMDs)

$\int dx$

$\int d^2k_T$

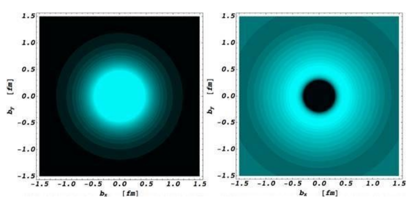

Form Factors
eg: $G_{E,}\ G_M$

Parton Distribution Functions (PDFs)

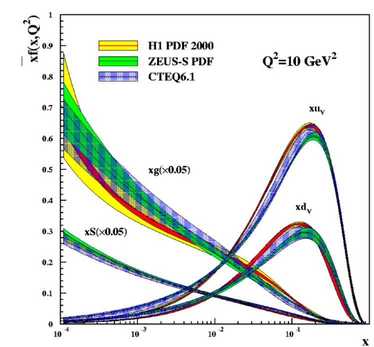

Images of the nucleon

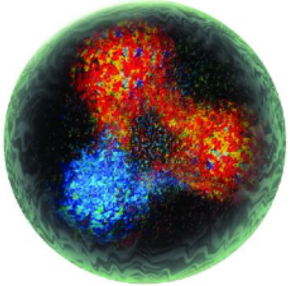

Wigner function:
full phase space parton distribution of the nucleon

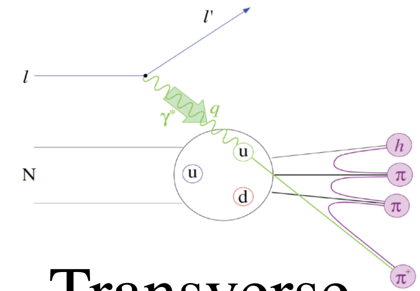

$\int d^2k_T$

$\int d^2b_T$

Transverse Momentum Distributions (TMDs)

Generalised Parton Distributions (GPDs)

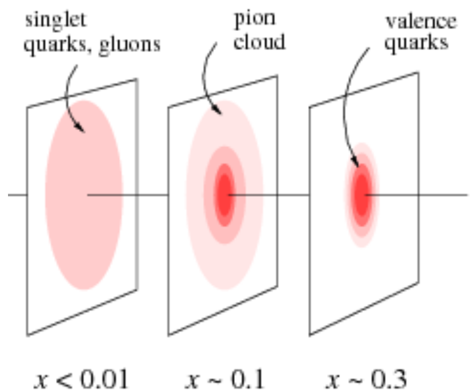

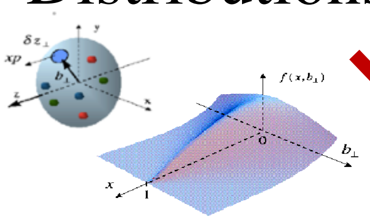

$\int dx$

$\int d^2k_T$

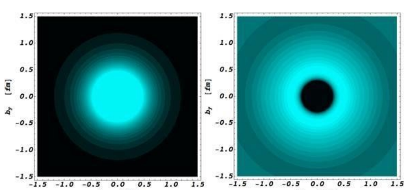

Form Factors
eg: G_{E}, G_{M}

Parton Distribution Functions (PDFs)

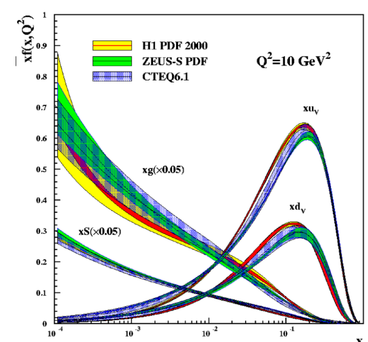

Generalised Parton Distributions (GPDs) —
proposed by Müller (1994), Radyushkin, Ji (1997).

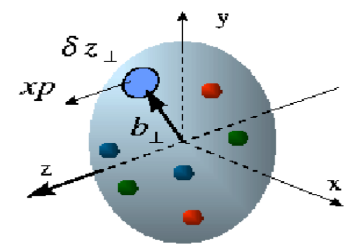

* *Directly related to the matrix element of the energy-momentum tensor evaluated between hadron states.*

In the infinite momentum frame, can be interpreted as relating transverse position of partons (impact parameter), $b_\perp$, to their longitudinal momentum fraction (x).

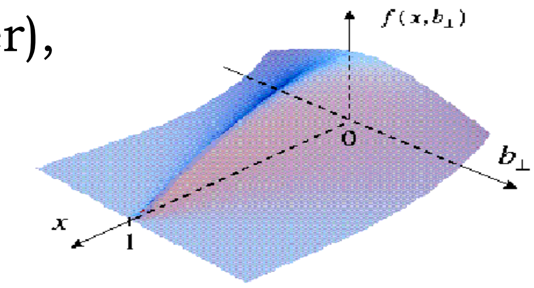

Tomography: 3D image of the nucleon.

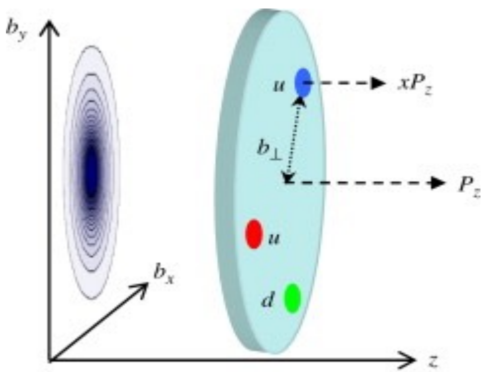

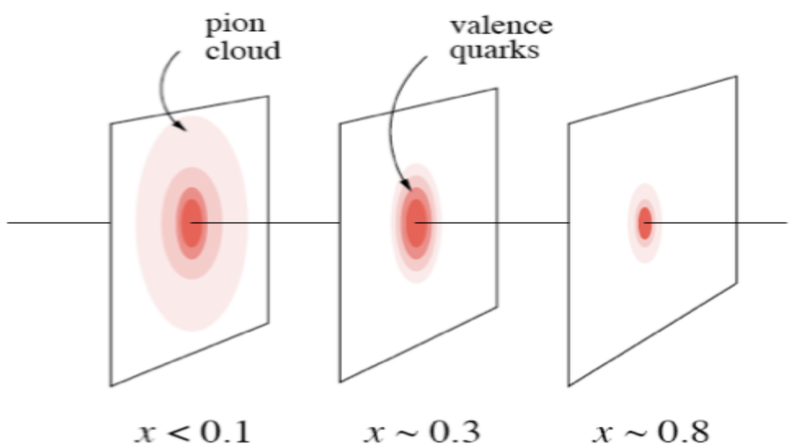

* First studies at JLab and DESY (HERMES), currently at JLab and CERN (COMPASS). A crucial part of the JLab12 programme — and, in the future, of the EIC.

Deeply Virtual Compton scattering

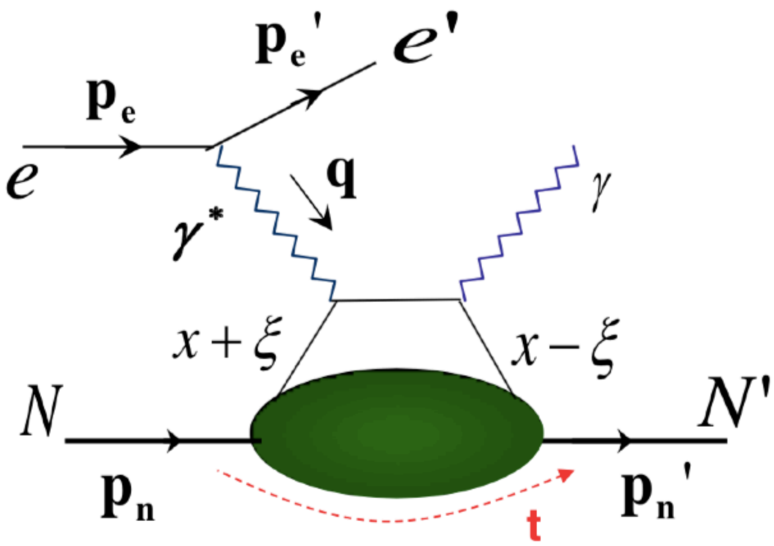

- $Q^2 = -\mathbf{q}^2 = -(\mathbf{p_e} - \mathbf{p_e}')^2$

  $\boldsymbol{q}$: four-momentum transfer to the struck quark

- $t = (\mathbf{p_n} - \mathbf{p}_n')^2 \qquad \nu = E_e - E_e'$

  t: quantifies change in four-momentum of the nucleon

- Bjorken variable $x_B = \dfrac{Q^2}{2\mathbf{p_n}\cdot\mathbf{q}}$

In the Bjorken limit (high Q^2, high ν), low t and infinite-nucleon-momentum frame:

- Skewness:

$$\xi \cong \frac{x_B}{2 - x_B}$$

- $x+\xi$ and $x-\xi$:

initial and final longitudinal momentum of struck quark, as a fraction of nucleon momentum

- Factorisation: allows to separate the "hard"-scattering of electron off a quark from the "soft" part of the interaction inside the nucleon.

"hard" interaction: perturbative calculation

"soft" interaction: parameterised by GPDs

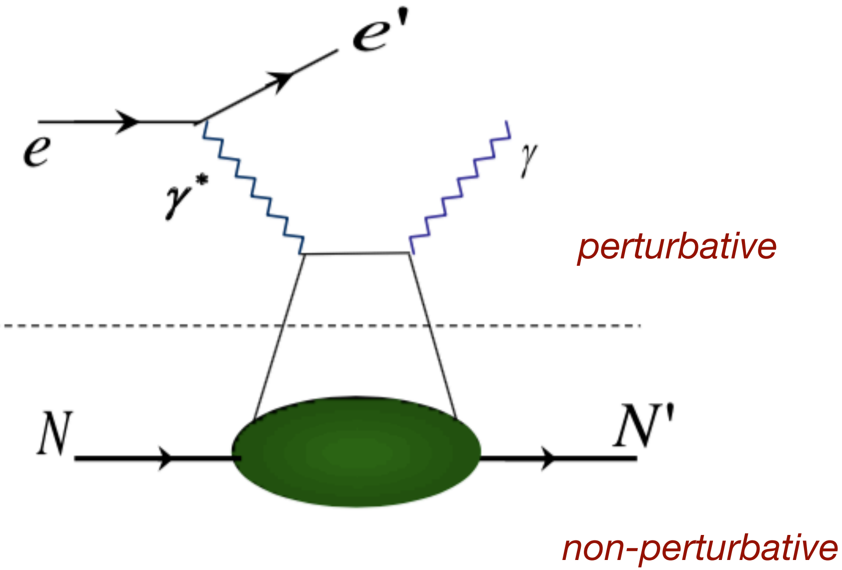

Factorisation only valid at high Q^2

$$E_q, \widetilde{E}_q, H_q, \widetilde{H}_q \; (x, \xi, t)$$

At leading order, leading twist four GPDs for each quark-flavour q

- At sufficiently high Q^2, can extract GPD information from cross-sections and asymmetries in DVCS and related processes.

Definitions: Order and Twist

- Twist: powers of $\frac{1}{\sqrt{Q^2}}$ in the DVCS amplitude. Leading-twist (LT) is twist-2.

- Order: introduces powers of α_s

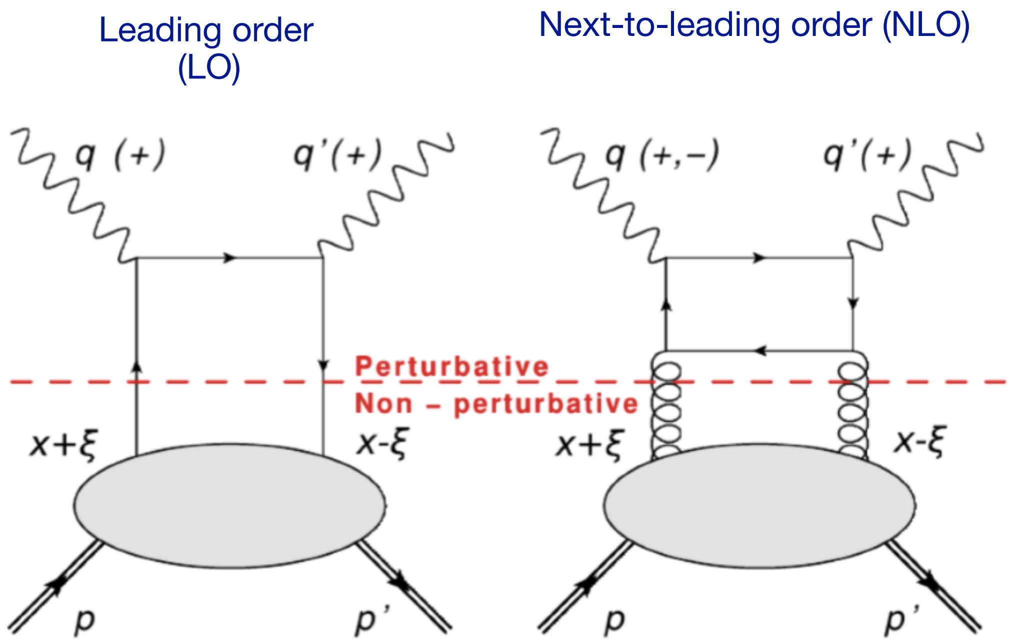

- LO requires $Q^2 >> M^2$ (M: target mass)

A closer look at GPDs

$$\left.\begin{array}{l} H(x,\xi,t): \\ E(x,\xi,t): \end{array}\right\}$$

Independent of quark helicity, unpolarised GPDs

$$\left.\begin{array}{l} \widetilde{H}(x,\xi,t): \\ \widetilde{E}(x,\xi,t): \end{array}\right\}$$

Helicity-dependent, polarised GPDs

If no longitudinal momentum transfer to quark ($\xi=0$) and no net momentum transfer to nucleon ($t=0$):

$$H(x,0,0) = q(x)$$
$$\widetilde{H}(x,0,0) = \Delta q(x)$$

→ Two of the GPDs reduce to PDFs

A closer look at GPDs

* The first Mellin moments of the GPDs reduce to Form Factors:

$$\int_{-1}^{1} dx\, H(x,\xi,t) = F_1(t) \qquad \int_{-1}^{1} dx\, \widetilde{H}(x,\xi,t) = G_A(t)$$

$$\int_{-1}^{1} dx\, E(x,\xi,t) = F_2(t) \qquad \int_{-1}^{1} dx\, \widetilde{E}(x,\xi,t) = G_P(t)$$

* Two distinct regions:

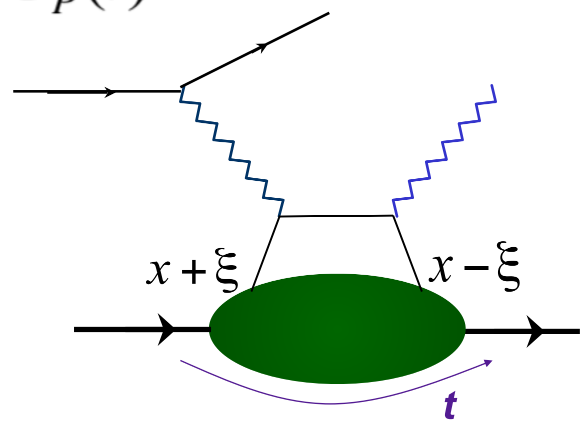

$|x| > |\xi|$ *The DGLAP region: scattering from quarks or anti-quarks*

$|x| < |\xi|$ *The ERBL region: scattering results in a $q\bar{q}$ pair.*

$t = \Delta^2$

* Fourier Transform of GPD w.r.t. Δ gives the transverse spatial distribution at each given *x*. Small changes in transverse momentum carry sensitivity to transverse structure at large distances within the nucleon.

The Nucleon Spin Puzzle

✳ What contributes to nucleon spin?

✳ 1980's: European Muon Collaboration (EMC) measures contribution of valence quarks to proton spin to be ~ 30 %. Subsequent deep inelastic scattering (DIS) experiments confirm.

Where is the rest? → **Proton spin crisis!**

Quark spin: extracted from helicity distributions measured in polarised DIS.

Gluon spin and OAM: measurements of DIS and polarised proton collisions indicate gluon spin ΔG contribution is very small, although in a different decomposition.

$$J_N = \frac{1}{2} = \frac{1}{2}\Sigma_q + L_q + J_g$$

Quark orbital angular momentum (OAM): can be accessed, in Ji's decomposition, via **GPDs**, which contain information on total angular momentum, J_q.

Caveat:

In Ji's decomposition of nucleon spin, the gluon spin and OAM terms cannot be separated.

GPDs and nucleon spin

$$J_N = \frac{1}{2} = \frac{1}{2}\Sigma_q + L_q + J_g$$

* Ji's relation: $J^q = \frac{1}{2} - J^g = \frac{1}{2}\int_{-1}^{1} x dx \left\{ H^q(x,\xi,0) + E^q(x,\xi,0) \right\}$

Second Mellin moments of the GPDs contain information on the total angular momentum carried by quarks.

Note that the contribution from GPD *H* is given by the quark momentum, already known from PDFs:

$$2J^q = \int_0^1 \mathrm{d}x\, x[q(x) + \bar{q}(x)] + \int_{-1}^{+1} \mathrm{d}x\, x E^q(x,0,0)$$

Experimental paths to GPDs

cliparts.co

Accessible in *exclusive* reactions, where all final state particles are detected.

Trodden paths, or ones starting to be explored:

- Deeply Virtual Compton Scattering (DVCS)
- Deeply Virtual Meson Production (DVMP)
- Time-like Compton Scattering (TCS)
- Double DVCS

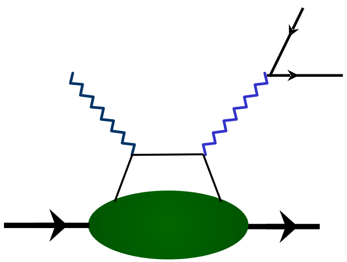

TCS

Virtual photon time-like

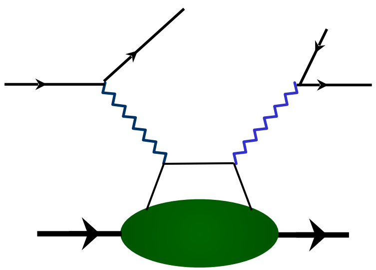

DDVCS

One time-like, one space-like virtual photon

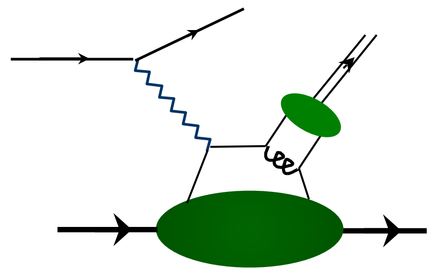

DVMP

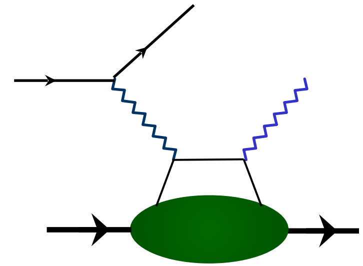

DVCS

Virtual photon space-like

Measuring DVCS

* Process measured in experiment:

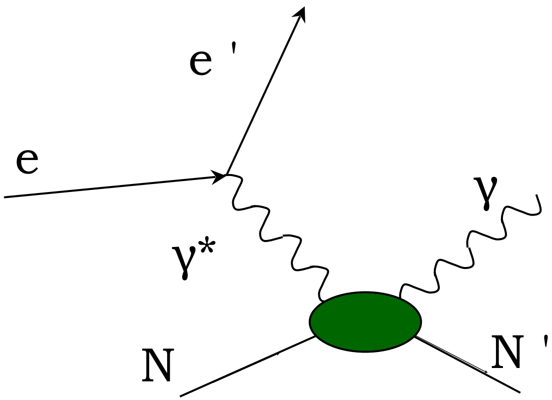

DVCS

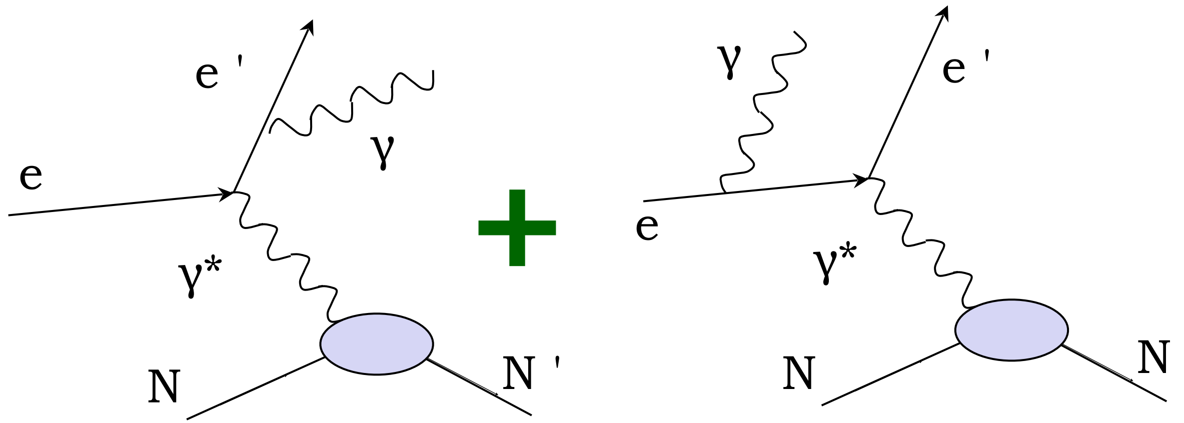

Bethe - Heitler

$$d\sigma \propto \left|T_{DVCS}\right|^2 + \left|T_{BH}\right|^2 + T_{BH}T^*{}_{DVCS} + T_{DVCS}T^*{}_{BH}$$

Amplitude parameterised in terms of Compton Form Factors

Amplitude calculable from elastic Form Factors and QED

Interference term

$$\left|T_{DVCS}\right|^2 << \left|T_{BH}\right|^2$$

Compton Form Factors in DVCS

Experimentally, DVCS amplitude is proportional to Compton Form Factors (CFFs) — sums of GPD integrals over *x*:

$$\int_{-1}^{1} dx F(\mp x, \xi, t) \left[\frac{1}{x - \xi + i\epsilon} \pm \frac{1}{x + \xi - i\epsilon} \right]$$

GPD

Plus sign for unpolarised GPDs, minus for polarised.

Can be decomposed into real and imaginary parts:

Cauchy's principal value integral

$$\Re e \mathcal{F} = \mathcal{P} \int_{-1}^{1} dx \left[\frac{1}{x - \xi} \mp \frac{1}{x + \xi} \right] F(x, \xi, t)$$

$$\Im m \mathcal{F}(\xi, t) = -\pi [F(\xi, \xi, t) \mp F(-\xi, \xi, t)]$$

- Both parts are accessible in different experimental observables

Compton Form Factors in DVCS

At leading twist, leading order:

$$T^{DVCS} \sim \int_{-1}^{+1} \frac{GPDs\,(x,\xi,t)}{x \pm \xi + i\varepsilon} dx + \ldots \sim \quad P\int_{-1}^{+1} \frac{GPDs\,(x,\xi,t)}{x \pm \xi} dx \pm i\pi GPDs\,(\pm\xi,\xi,t) + \ldots$$

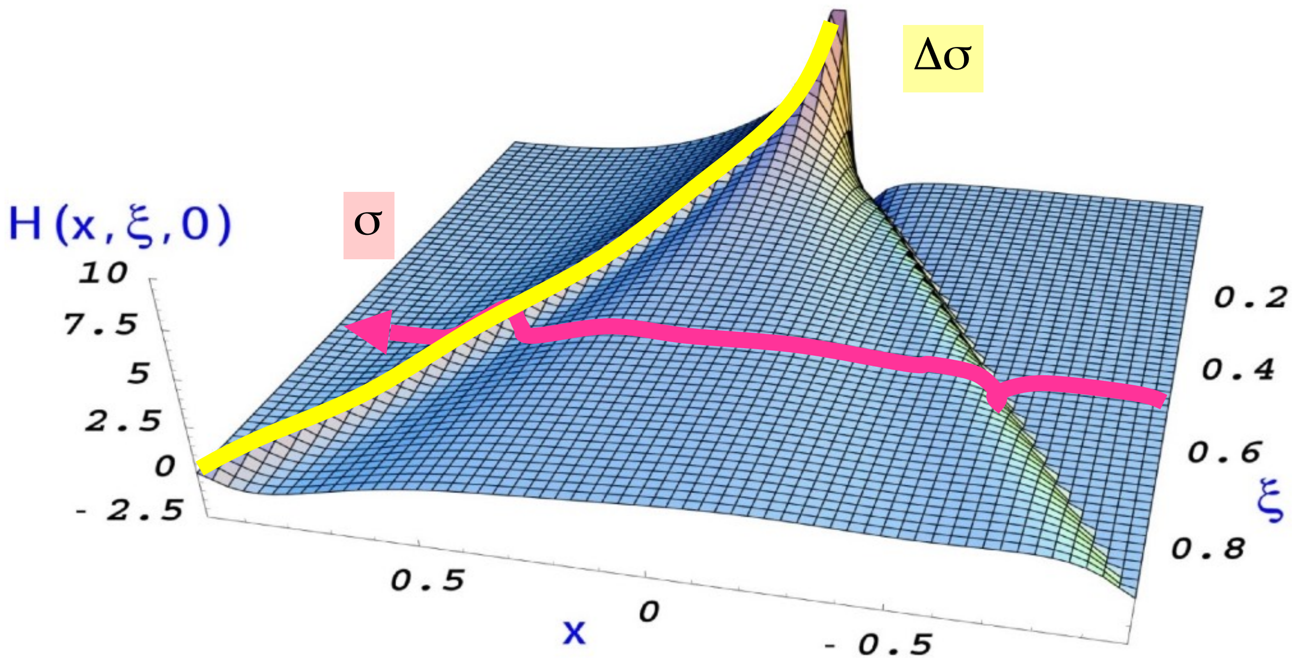

Only ξ and t are accessible experimentally!

To get information on x need extensive measurements in Q^2.

Need measurements off proton and neutron to get flavour separation of CFFs in DVCS.

DVCS kinematics and observables

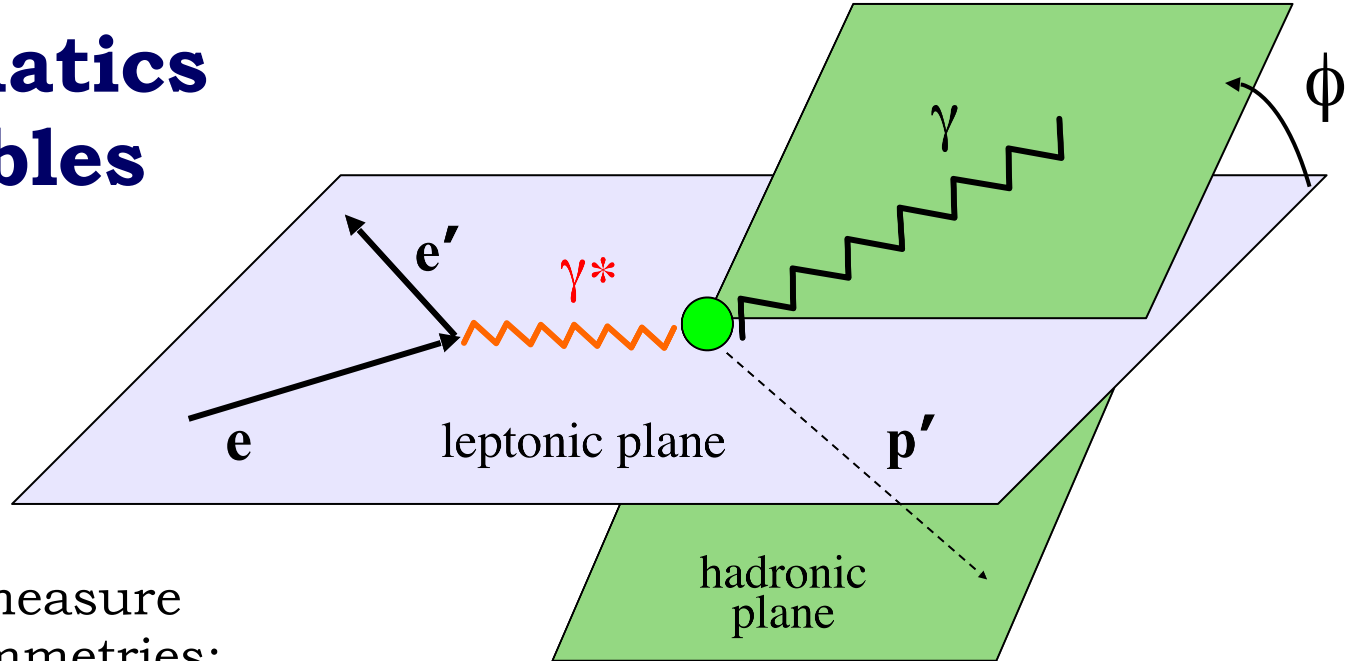

Experimentally, can measure cross-sections or asymmetries:

$$A = \frac{d\vec{\sigma} - d\overleftarrow{\sigma}}{d\vec{\sigma} + d\overleftarrow{\sigma}} = \frac{\Delta\sigma}{d\vec{\sigma} + d\overleftarrow{\sigma}}$$

- Beam-charge asymmetry, from a probe with two opposite charges (e^+/e^-)
- Beam-spin asymmetry, from different electron helicities
- Target-spin asymmetry, from different target polarisation orientations
- Double-spin asymmetries, from combining beam and target polarisations

Which DVCS experiment?

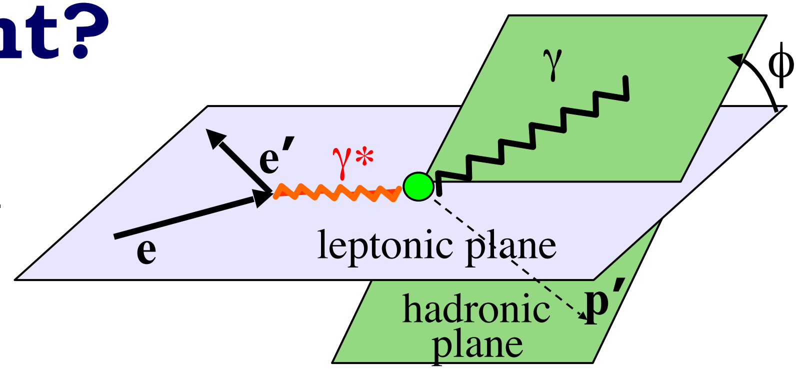

Real parts of CFFs accessible in cross-sections, beam-charge and double polarisation asymmetries,

imaginary parts of CFFs in single-spin asymmetries.

Beam, target polarisation

For example:

Proton | Neutron

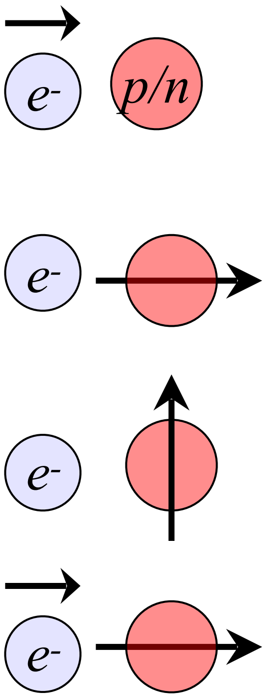

$$\Delta\sigma_{LU} \sim \sin\phi \, \Im(F_1 H + \xi G_M \tilde{H} - \frac{t}{4M^2} F_2 E)\, d\phi$$

$\rightarrow$ $Im\{\boldsymbol{H_p}, \tilde{H}_p, E_p\}$, $Im\{H_n, \tilde{H}_n, \boldsymbol{E_n}\}$

$$\Delta\sigma_{UL} \sim \sin\phi \, \Im(F_1 \tilde{H} + \xi G_M (H + \frac{x_B}{2} E) - \xi \frac{t}{4M^2} F_2 \tilde{E} + \ldots)\, d\phi$$

$\rightarrow$ $Im\{\boldsymbol{H_p}, \boldsymbol{\tilde{H}_p}\}$, $Im\{\boldsymbol{H_n}, E_n, \tilde{E}_n\}$

$$\Delta\sigma_{UT} \sim \cos\phi \, \Im(\frac{t}{4M^2}(F_2 H - F_1 E) + \ldots) d\phi$$

$\rightarrow$ $Im\{\boldsymbol{H_p}, \boldsymbol{E_p}\}$, $Im\{\boldsymbol{H_n}\}$

$$\Delta\sigma_{LL} \sim (A + B\cos\phi)\, \Re(F_1 \tilde{H} + \xi G_M (H + \frac{x_B}{2} E) + \ldots) d\phi$$

$\rightarrow$ $Re\{\boldsymbol{H_p}, \boldsymbol{\tilde{H}_p}\}$, $Re\{\boldsymbol{H_n}, E_n, \tilde{E}_n\}$

Other reactions to get at GPDs

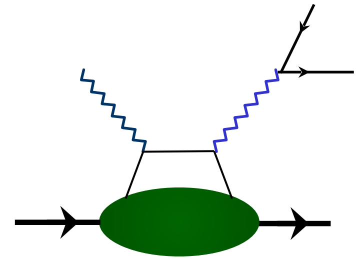

- **Time-like Compton scattering**: virtual photon is time-like. At leading order, access same integrals of GPDs. At higher orders, they differ.

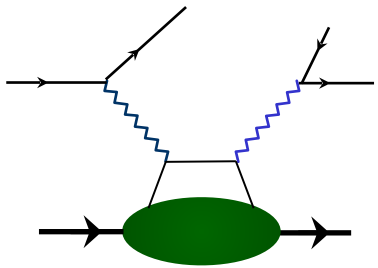

- **Double Deeply Virtual Compton scattering**: two virtual photons: the second vertex provides a second variable Q'^2. This allows direct access to x, but cross-sections are suppressed by another factor of α.

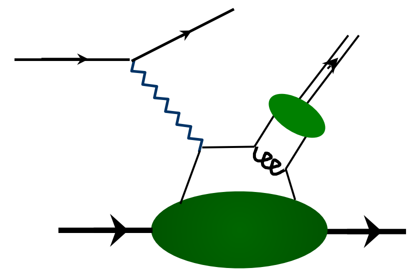

- **Deeply Virtual Meson Production**: the meson vertex provides flavour information. Amplitude now depends on GPDs and the meson Distribution Amplitudes. In light mesons, more sensitive to higher order and higher twist.

In vector mesons, gluon GPDs appear at lowest order!

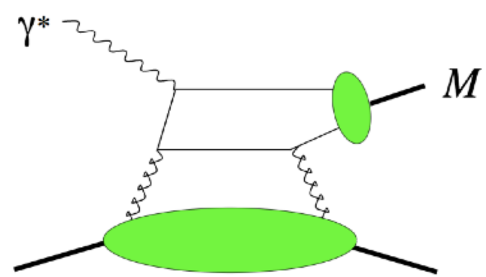

Deeply Virtual Meson Production

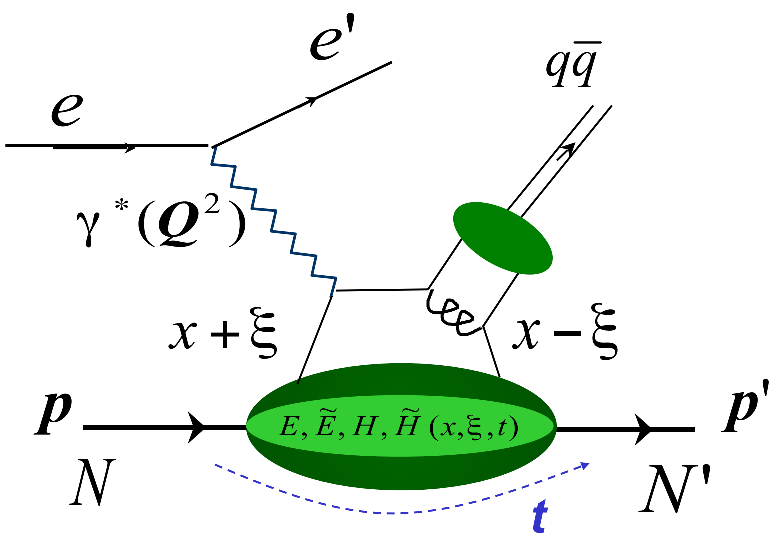

At leading order & twist, access to the four chirally even (parton helicity-conserving) GPDs:

* Pseudo-scalar mesons: $\tilde{H}^q, \tilde{E}^q(x,\xi,t)$

  eg: π, η mesons ($J^P = 0^-$)

* Vector mesons: $H^q, E^q, H^g, E^g(x,\xi,t)$

  eg: ρ, ω, ϕ mesons ($J^P = 1^-$)

Gluon GPDs!

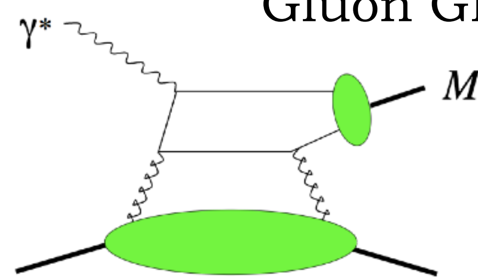

Additionally, one gains access to four chirally-odd (parton helicity-flipping) transversity GPDs:

$$E_T^q, \tilde{E}_T^q, H_T^q, \tilde{H}_T^q(x,\xi,t)$$

Plus, DVMP enables flavour decomposition of quark GPDs!

Transversity GPDs

* Transversity GPDs appear in the scattering amplitude when the virtual photon has a transverse polarisation.

Not accessible at leading twist in DVCS, but appearing in DVMP!

* $\tilde{E}_T$ can be related to the transverse anomalous magnetic moment:

$$\kappa_T = \int_{-1}^{+1} \tilde{E}_T(x, \xi, t=0)\, dx$$

* and H_T to the transversity distribution: $H_T(x, 0, 0) = h_1(x)$

which describes distribution of transverse partons in a transverse nucleon

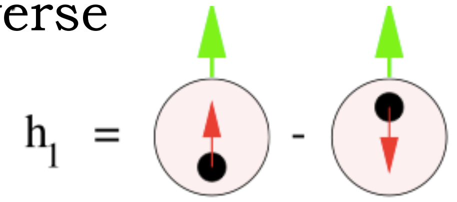

* The combination $\bar{E}_T = 2\tilde{H}_T + E_T$

is related to spatial density of transversely polarised quarks in an unpolarised nucleon.

DVMP Cross-section

Virtual
photon flux

unpolarised

$$\frac{2\pi}{\Gamma}\frac{d^4\sigma}{dQ^2 dx_B dt d\phi_{meson}} = \boxed{\sigma_T + \epsilon\sigma_L + \epsilon\sigma_{TT}\cos 2\phi + \sqrt{\epsilon(1+\epsilon)}\sigma_{LT}\cos\phi}$$

longitudinally polarised beam

$$\boxed{+P_b\sqrt{\epsilon(1-\epsilon)}\sigma_{LT'}\sin\phi}$$

longitudinally polarised target

$$\boxed{+P_{tg}\left(\sqrt{\epsilon(1+\epsilon)}\sigma_{UL}^{\sin\phi}\sin\phi + \epsilon\sigma_{UL}^{\sin 2\phi}\sin 2\phi\right)}$$

Target and beam longitudinally polarised

$$\boxed{+P_b P_{tg}\left(\sqrt{1-\epsilon^2}\sigma_{LL} + \sqrt{\epsilon(1-\epsilon)}\sigma_{LL}^{\cos\phi}\cos\phi\right)}$$

where $\epsilon = \dfrac{1 - y - \frac{Q^2}{4E^2}}{1 - y + \frac{y^2}{2} + \frac{Q^2}{4E^2}}$ is the ratio of the fluxes of longitudinally (L) and transversely (T) polarised virtual photons and

$$y = pq/qk = \nu/E$$

DVMP Cross-sections

* Unpolarised cross-section for meson-production:

$$\frac{d^2\sigma}{dt\,d\phi_\pi} = \frac{1}{2\pi}\left[\left(\frac{d\sigma_T}{dt} + \epsilon\frac{d\sigma_L}{dt}\right) + \epsilon\cos 2\phi_\pi\frac{d\sigma_{TT}}{dt} + \sqrt{2\epsilon(1+\epsilon)}\cos\phi_\pi\frac{d\sigma_{LT}}{dt}\right]$$

* Structure functions which parametrise the cross-section are related to scattering amplitudes in the interaction thus:

$$\frac{d\sigma_i}{dt} = \frac{1}{16\pi}\frac{x_B^2}{1-x_B}\frac{1}{Q^4}\frac{1}{\sqrt{1+4x_B^2m^2/Q^2}}\sum_{\text{spins}}{}' \left|\mathcal{A}(\gamma_i^* p \to M p)\right|^2$$

$i = T, L$

DVMP Cross-sections and GPDs

Relation between structure functions in DVMP and GPDs:

$$\frac{d\sigma_L}{dt} = \frac{4\pi\alpha}{k'}\frac{1}{Q^6}\left\{(1-\xi^2)|\langle\tilde{H}\rangle|^2 - 2\xi^2\mathrm{Re}[\langle\tilde{H}\rangle^*\langle\tilde{E}\rangle] - \frac{t'}{4m^2}\xi^2|\langle\tilde{E}\rangle|^2\right\}$$

$$\frac{d\sigma_T}{dt} = \frac{4\pi\alpha}{2k'}\frac{\mu_\pi^2}{Q^8}\left[(1-\xi^2)|\langle H_T\rangle|^2 - \frac{t'}{8m^2}|\langle\bar{E}_T\rangle|^2\right]$$

$$\frac{d\sigma_{LT}}{dt} = \frac{4\pi\alpha}{\sqrt{2}k'}\frac{\mu_\pi}{Q^7}\xi\sqrt{1-\xi^2}\frac{\sqrt{-t'}}{2m}\mathrm{Re}[\langle H_T\rangle^*\langle\tilde{E}\rangle]$$

$$\frac{d\sigma_{TT}}{dt} = \frac{4\pi\alpha}{k'}\frac{\mu_\pi^2}{Q^8}\frac{t'}{16m^2}|\langle\bar{E}_T\rangle|^2$$

where $\langle F\rangle \equiv \sum_\lambda \int_{-1}^{1} dx\,\mathcal{H}_{\mu'\lambda'\mu\lambda} F$.

$$\bar{E}_T = 2\tilde{H}_T + E_T$$

Hard-scattering kernel for quark (λ, λ'), photon (μ) and meson (μ') helictites

GPD

Nucleon Tomography from GPDs

- At a fixed Q^2, x_B, slope of GPD with t is related, via a Fourier Transform, to the transverse spatial spread.

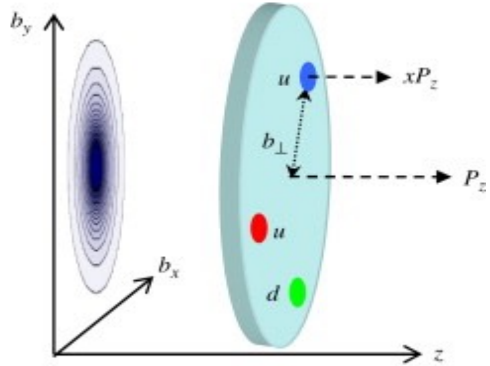

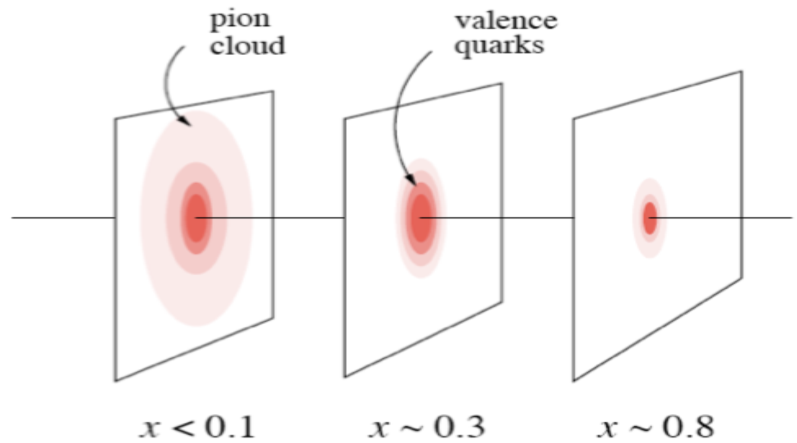

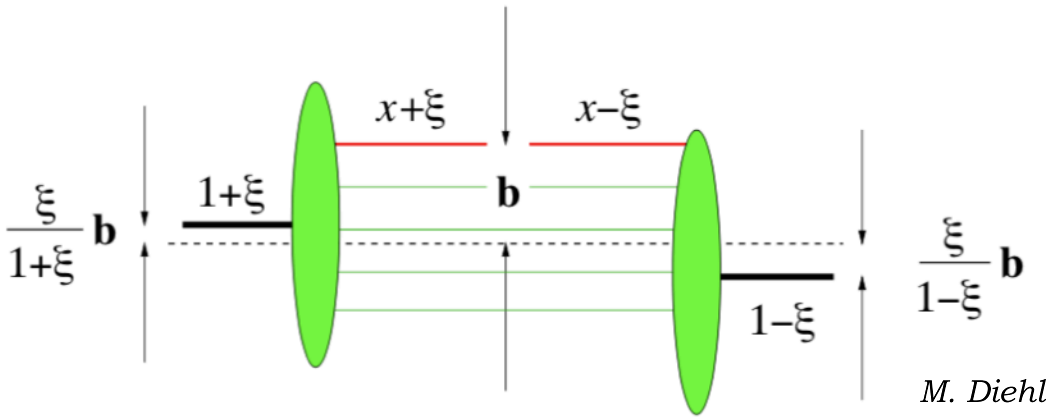

Formally, the radial separation, **b**, *between the struck parton and the centre of momentum of the remaining spectators.*

- Experimentally, fit the t-dependence of structure functions or CFFs with an exponential.

eg: $$\frac{d\sigma_U}{dt} = Ae^{Bt}$$

Nucleon Tomography from GPDs

* Flavour separation is possible in DVCS using different targets (proton and neutron), and in DVMP with different mesons.

For example, compare measurements of π^0 and η DVMP:

$$H_T^{\pi^0} = (e_u H_T^u - e_d H_T^d)/\sqrt{2}, \qquad H_T^{\eta} = (e_u H_T^u + e_d H_T^d)/\sqrt{6},$$

$$\bar{E}_T^{\pi^0} = (e_u \bar{E}_T^u - e_d \bar{E}_T^d)/\sqrt{2}, \qquad \bar{E}_T^{\eta} = (e_u \bar{E}_T^u + e_d \bar{E}_T^d)/\sqrt{6}.$$

Up-quark charge

(Goloskokov-Kroll model)

* Different GPDs represent different aspects of the parton distributions: EM charge, axial charge, transversity, etc….

* Sensitivity to gluon distributions through gluon GPDs.

Particularly cleanly accessible for heavier q: J/Ψ

Measuring DVCS/DVMP

- Need an exclusive reconstruction of the reaction, eg. DVCS:

Known from the accelerator

Known from the target / accelerator

Need to detect

$$ep \to e'p'\gamma$$

Either detect or reconstruct through missing mass techniques

Similarly for DVMP

Must be detected

- HERMES @ DESY: electron / positron scattering on fixed gas target
- COMPASS @ CERN: muon scattering on fixed targets
- **JLab (6 and 11 GeV):** electron (positron?) scattering on fixed targets
- EIC: electron / positron - proton / ion collisions

Jefferson Lab today

CEBAF: Continuous Electron Beam Accelerator Facility.

- Energy up to 11 GeV (Halls A, B, C), 12 GeV Hall D
- Energy spread $\delta E/E_e \sim 10^{-4}$
- Electron polarisation up to >80%, measured to 3%
- Beam size at target < 0.4 mm

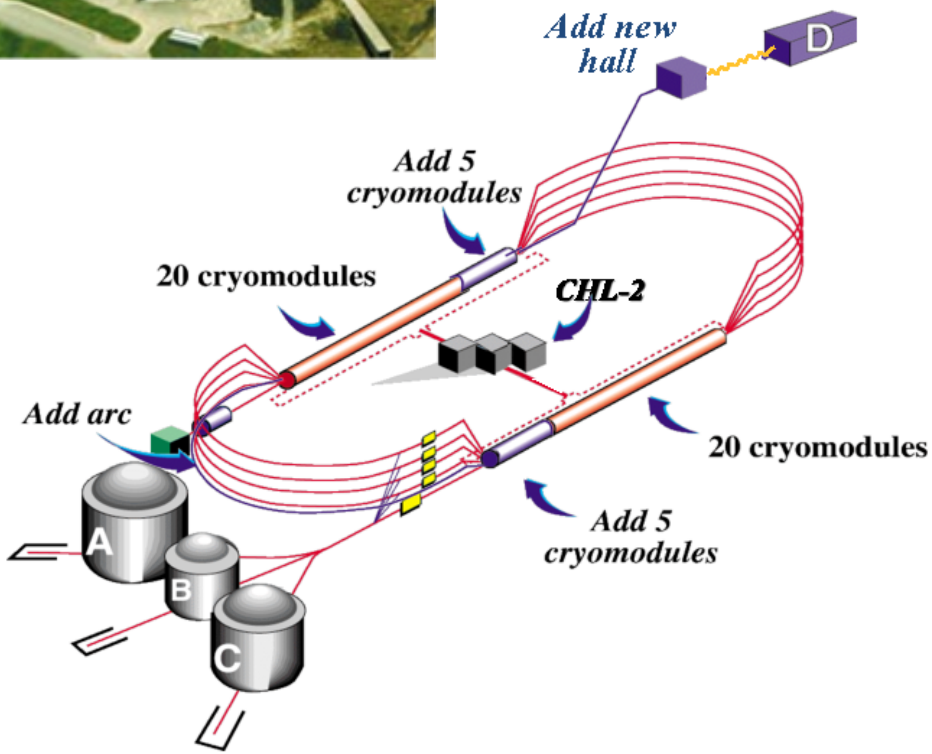

Jefferson Lab: 6 GeV era

CEBAF: Continuous Electron Beam Accelerator Facility.

- Energy up to ~6 GeV
- Energy resolution $\delta E/E_e \sim 10^{-5}$
- Longitudinal electron polarisation up to ~85%

Hall A:

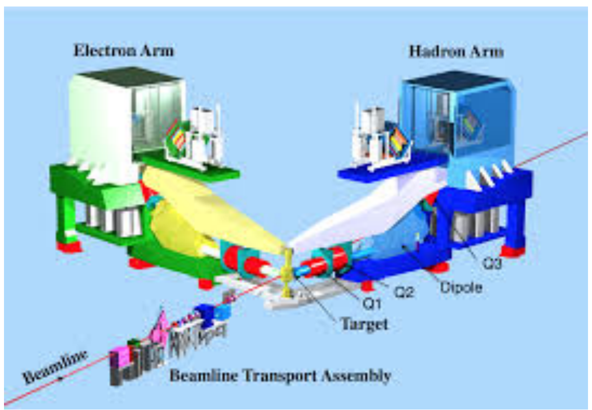

- High resolution($\delta p/p = 10^{-4}$) spectrometers, very high luminosity.

Hall B: CLAS

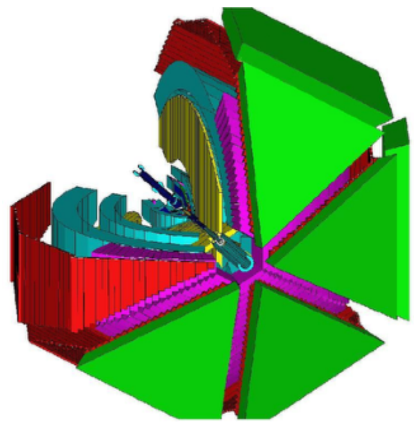

- Very large acceptance, detector array for multi-particle final states.

Hall C:

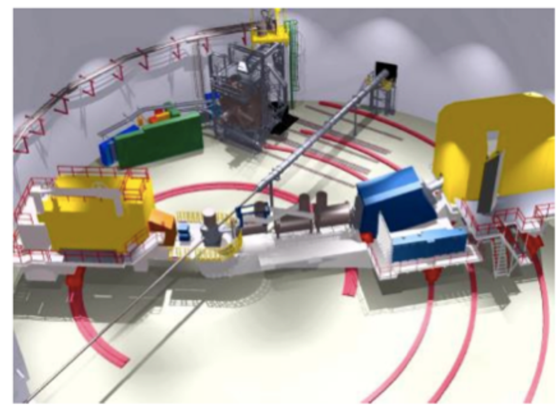

- Two movable spectrometer arms, well-defined acceptance, high luminosity

CLAS in Hall B: 6 GeV era

- ❖ Drift chambers
- ❖ Toroidal magnetic field
- ❖ Cerenkov Counters
- ❖ Scintillator Time of Flight
- ❖ Electromagnetic Calorimeters

+ a forward-angle Inner Calorimeter:

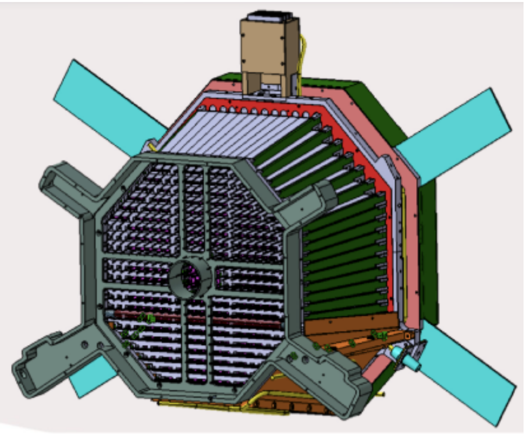

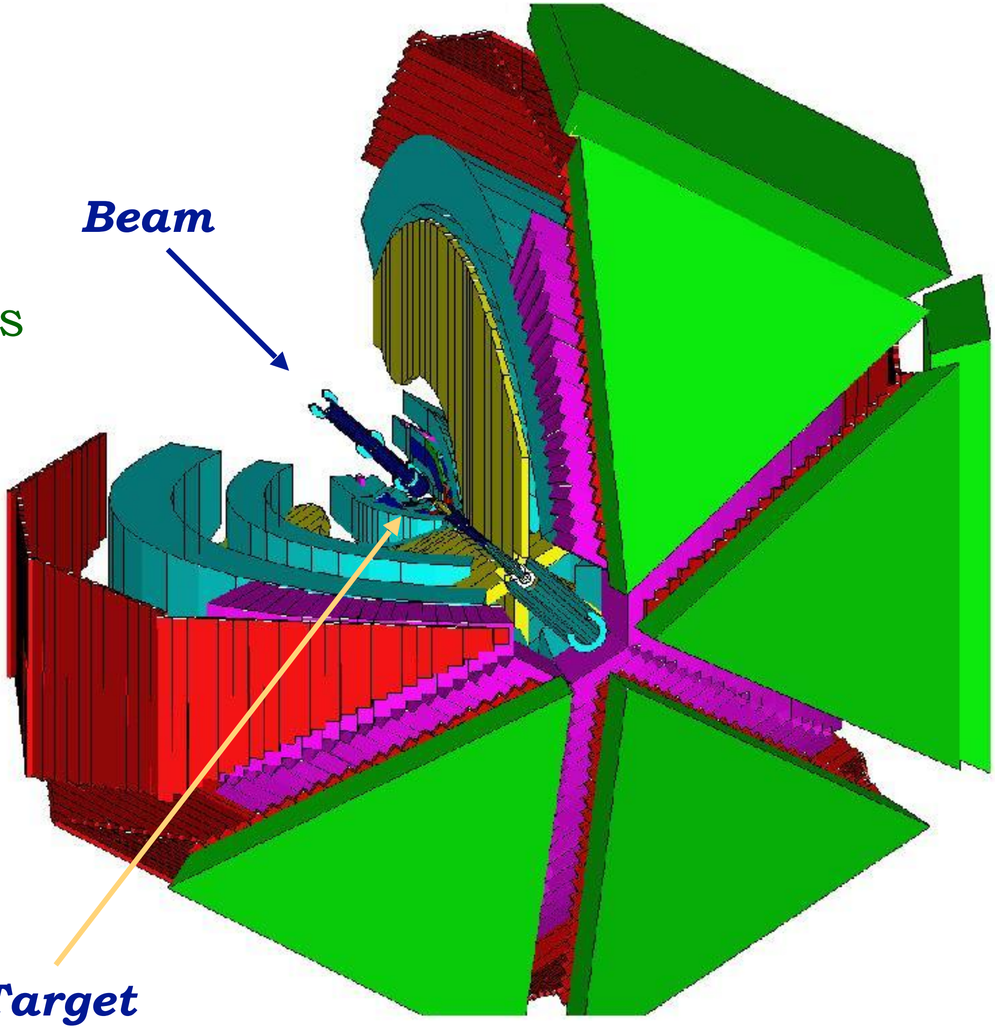

Charged particle ID in CLAS

- **Charge**: direction of track curvature through drift chambers in toroidal magnetic field
- **Momentum**: radius of curvature
- **Time of flight**: from beam bunch timing and thin scintillator paddles beyond the drift chambers - combine with track length to give β

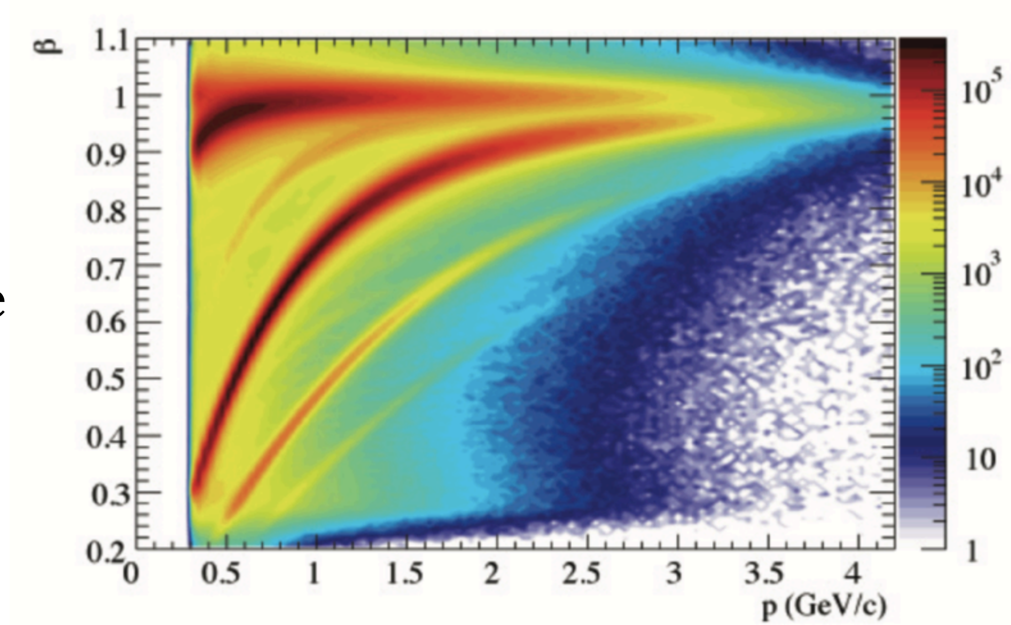

G. Smith Thesis

$$m^2 = \frac{p^2(1-\beta^2)}{\beta^2}$$

- Works well to ID heavy species. Need more tricks for light ones!

Electrons and π^- in CLAS

- Electrons leave a signal in Cerenkov Counters: pions will not.
- Energy deposit in the Electromagnetic Calorimeter (EC).

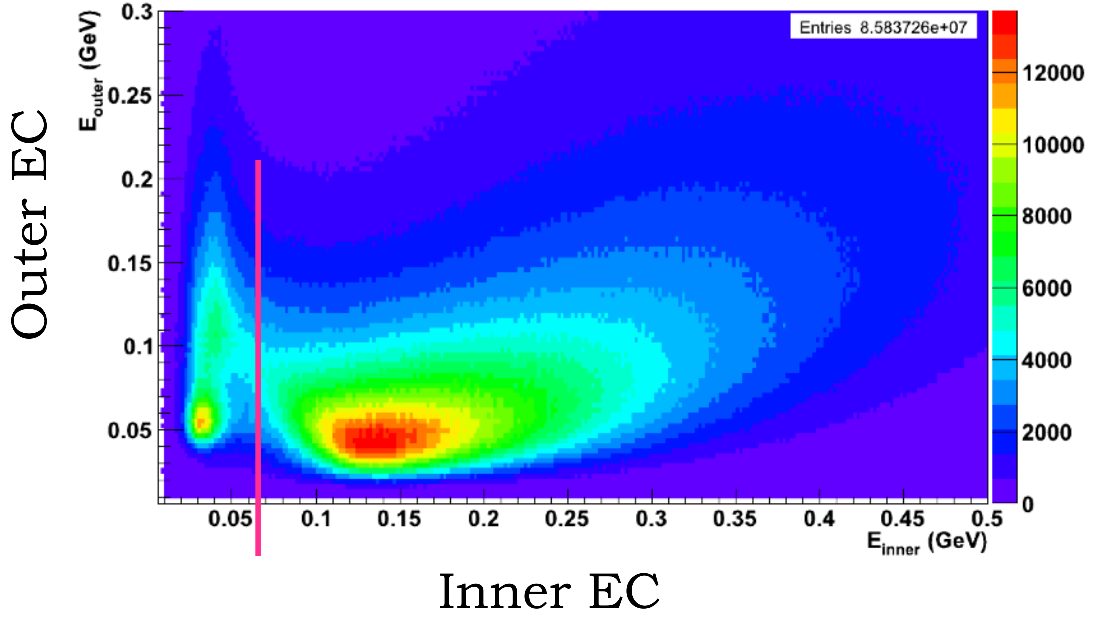

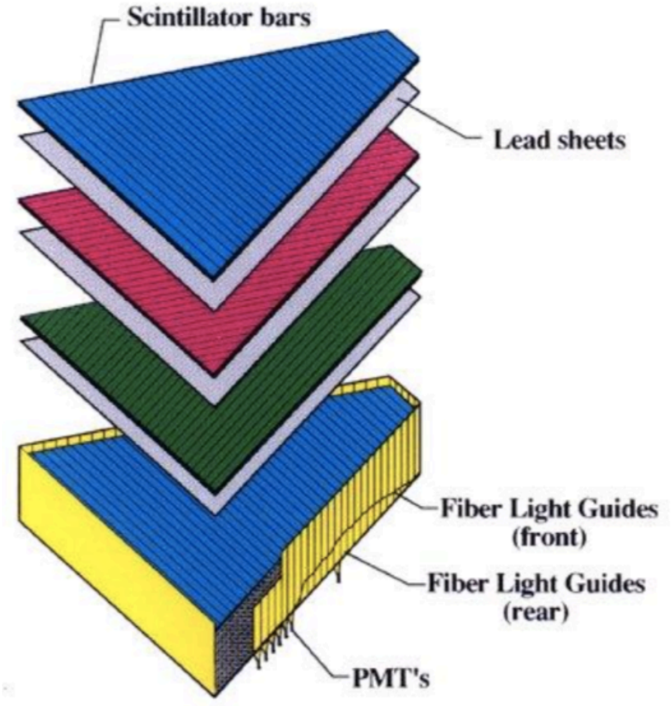

Neutrals: photons, neutrons, π^0

- Energy deposit in the calorimeters + lack of charged track.
- Photons in the EC and IC (very forward angles), neutrons only in EC.
- Can reconstruct π^0 through invariant mass.

$$m_{\pi^0} = 0.135\,\mathrm{GeV/c^2}$$

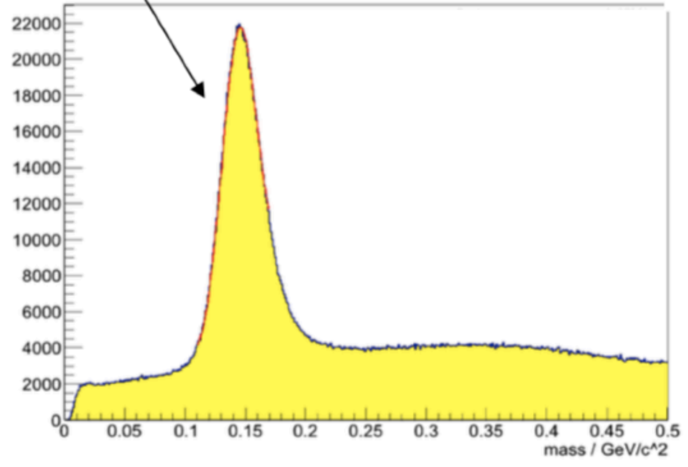

Targets for CLAS

- Unpolarised protons: Liquid H_2
- Longitudinally polarised protons: Frozen ammonia beads (NH_3)

- Unpolarised neutrons: Liquid D_2
- Longitudinally polarised neutrons: Frozen deuterated ammonia beads (ND_3)

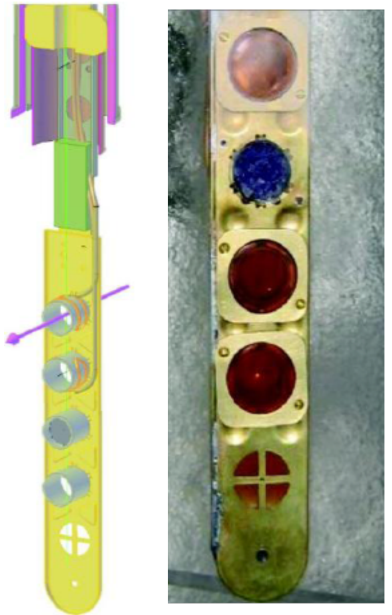

Eg1-dvcs target

- Dynamic Nuclear Polarisation (DNP): polarise butanol or ammonia in a high magnetic field (5T) at low temp (1K), use microwaves to transfer electron polarisation to protons/deuterons.

- Transverse target polarisation possible, but very challenging…

In the CLAS era: FROST, HD-ice (but only for photon beams)

Reconstructing the DVCS reaction

- A series of experiment-dependent "exclusivity cuts" to ID reaction.
  Example from eg1-dvcs (CLAS):

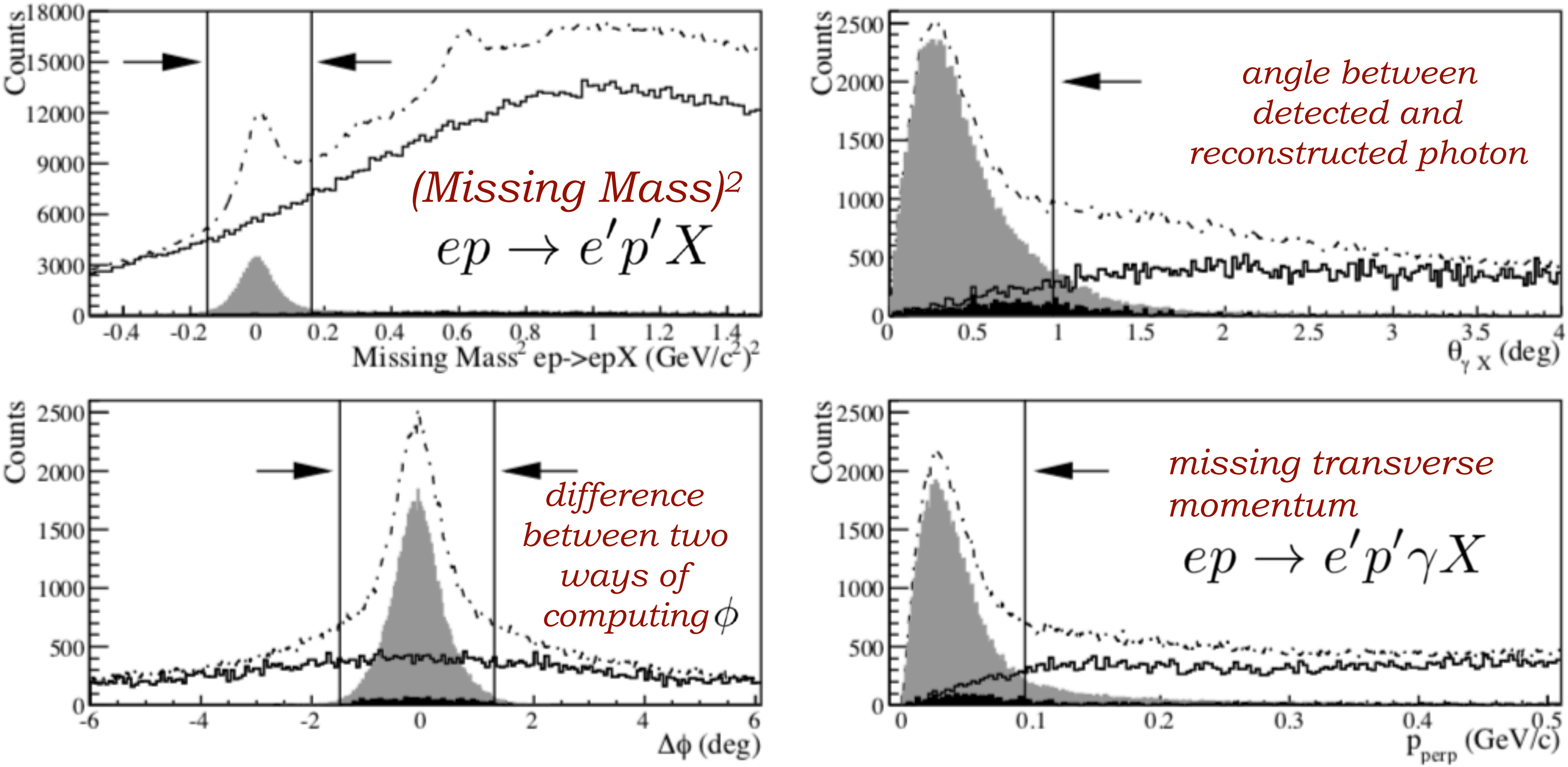

Lines: before exclusivity cuts (dashed: NH_3, solid: C)
Filled: after (grey: signal, black: background), arrows indicate cut.

S. Pisano *et al* (CLAS), ***PRD* 91** (2015) 052014

DVCS asymmetries @ CLAS

The "eg1-dvcs" experiment.

- Feb. - Sept. 2009
- 5.87 and 5.95 GeV polarised electron beam
- Longitudinally polarised (via DNP) $^{14}NH_3$ target, 1.45 cm long, 1.5cm diam.
- CLAS + Inner Calorimeter detectors
- Exclusive reconstruction:

$$ep \rightarrow e'p'\gamma$$

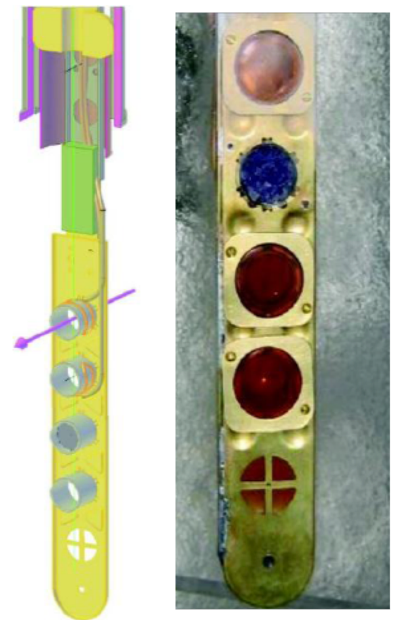

Eg1-dvcs target

Extracting asymmetries

Number of DVCS/BH events for each kinematic bin:

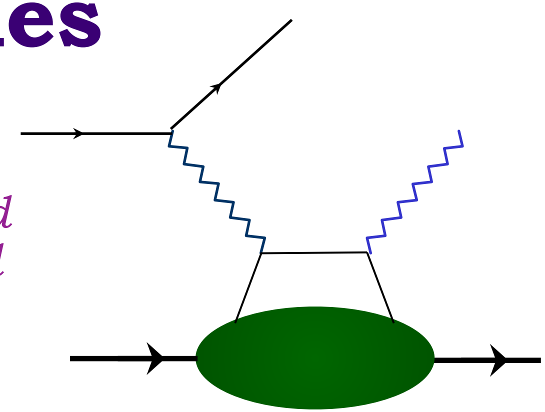

$$N^{bt} = (1 - B^{bt}_{\pi^0}) \cdot \frac{N^{bt}_{ep\gamma}}{FC^{bt}}$$

Number of detected events in identified reaction

Polarisation state of beam, target

Background due to π^0 contamination

Normalisation by beam current (in Faraday Cup)

- Beam-spin asymmetry:

$$A_{\mathrm{LU}} = \frac{P_t^-(N^{++} - N^{-+}) + P_t^+(N^{+-} - N^{--})}{P_b(P_t^-(N^{++} + N^{-+}) + P_t^+(N^{+-} + N^{--}))}$$

Beam, target polarisation

- Target-spin asymmetry:

$$A_{\mathrm{UL}} = A^{\mathrm{lab}}_{\mathrm{UL}} + c_{A_{\mathrm{UT}}}$$

Correction for electron / virtual photon axes

$$A^{\mathrm{lab}}_{\mathrm{UL}} = \frac{N^{++} + N^{-+} - N^{+-} - N^{--}}{D_f(P_t^-(N^{++} + N^{-+}) + P_t^+(N^{+-} + N^{--}))}$$

Dilution factor due to unpolarised background

- Double-spin asymmetry:

$$A_{\mathrm{LL}} = A^{\mathrm{lab}}_{\mathrm{LL}} + c_{A_{\mathrm{LT}}}$$

$$A^{\mathrm{lab}}_{\mathrm{LL}} = \frac{N^{++} + N^{--} - N^{+-} - N^{-+}}{P_b \cdot D_f(P_t^-(N^{++} + N^{-+}) + P_t^+(N^{+-} + N^{--}))}$$

The DVCS/BH amplitude

$$\mathcal{T}^2 = |\mathcal{T}_{\rm BH}|^2 + |\mathcal{T}_{\rm DVCS}|^2 + \mathcal{I}$$

Interference term for DVCS/BH

$$|\mathcal{T}_{\rm BH}|^2 = \frac{e^6}{x_B^2 y^2 (1+\epsilon^2)^2 t\, \mathcal{P}_1(\phi)\mathcal{P}_2(\phi)} [c_0^{\rm BH} + \sum_{n=1}^{2} c_n^{\rm BH} \cos n\phi + s_1^{\rm BH} \sin\phi]$$

$$|\mathcal{T}_{\rm DVCS}|^2 = \frac{e^6}{y^2 \mathcal{Q}^2} \{c_0^{\rm DVCS} + \sum_{n=1}^{2} [c_n^{\rm DVCS} \cos n\phi + s_n^{\rm DVCS} \sin n\phi]\}$$

$$\mathcal{I} = \frac{e^6}{x_B y^3 t \mathcal{P}_1(\phi)\mathcal{P}_2(\phi)} \{c_0^{\mathcal{I}} + \sum_{n=1}^{3} [c_n^{\mathcal{I}} \cos n\phi + s_n^{\mathcal{I}} \sin n\phi]\}$$

Intermediate lepton propagators

Coefficients depending on Compton Form Factors

From asymmetries to CFFs

At leading twist, beam-spin asymmetry (BSA) can be expressed as:

$$A_{\mathrm{LU}}(\phi) \sim \frac{s^{\mathcal{I}}_{1,\mathrm{unp}} \sin\phi}{c^{\mathrm{BH}}_{0,\mathrm{unp}} + (c^{\mathrm{BH}}_{1,\mathrm{unp}} + c^{\mathcal{I}}_{1,\mathrm{unp}} + \ldots)\cos\phi \ldots}$$ *higher-twist terms…*

The leading coefficient is related to the imaginary part of the Compton Form Factors:

$$s^{\mathcal{I}}_{1,\mathrm{unp}} \propto \Im\mathrm{m}[F_1 \mathcal{H} + \xi(F_1 + F_2)\widetilde{\mathcal{H}} - \frac{t}{4M^2} F_2 \mathcal{E}]$$

At CLAS kinematics, this dominates

F_1, F_2: Dirac, Pauli form factors

Likewise, for the target-spin asymmetry (TSA):

$$A_{\mathrm{UL}}(\phi) \sim \frac{s^{\mathcal{I}}_{1,\mathrm{LP}} \sin\phi}{c^{\mathrm{BH}}_{0,\mathrm{unp}} + (c^{\mathrm{BH}}_{1,\mathrm{unp}} + c^{\mathcal{I}}_{1,\mathrm{unp}} + \ldots)\cos\phi + \ldots}$$

$$s_{1,\mathrm{LP}} \propto \Im\mathrm{m}[F_1 \widetilde{\mathcal{H}} + \xi(F_1 + F_2)(\mathcal{H} + \frac{x_B}{2}\mathcal{E}) - \xi(\frac{x_B}{2} F_1 + \frac{t}{4M^2} F_2)\widetilde{\mathcal{E}}]$$

At CLAS kinematics, these CFFs dominate

* Obtain coefficients from fitting the phi-dependence of the asymmetry:

$$A_i = \frac{\alpha_i \sin\phi}{1 + \beta_i \cos\phi}$$

Target-spin Asymmetry (A_{UL})

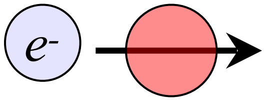

Follows first CLAS measurement:
S. Chen *et al* (CLAS),
***PRL* 97** (2006) 072002

A_{UL} from fit to asymmetry:

$$A_i = \frac{\alpha_i \sin\phi}{1 + \beta_i \cos\phi}$$

A_{UL} characterised by imaginary parts of CFFs via:

$$F_1 \tilde{H} + \xi G_M \left(H + \frac{x_B}{2} E \right) - \frac{\xi t}{4M^2} F_2 \tilde{E} + \ldots$$

High statistics, large kinematic coverage, strong constraints on fits, simultaneous fit with BSA and DSA from the same dataset.

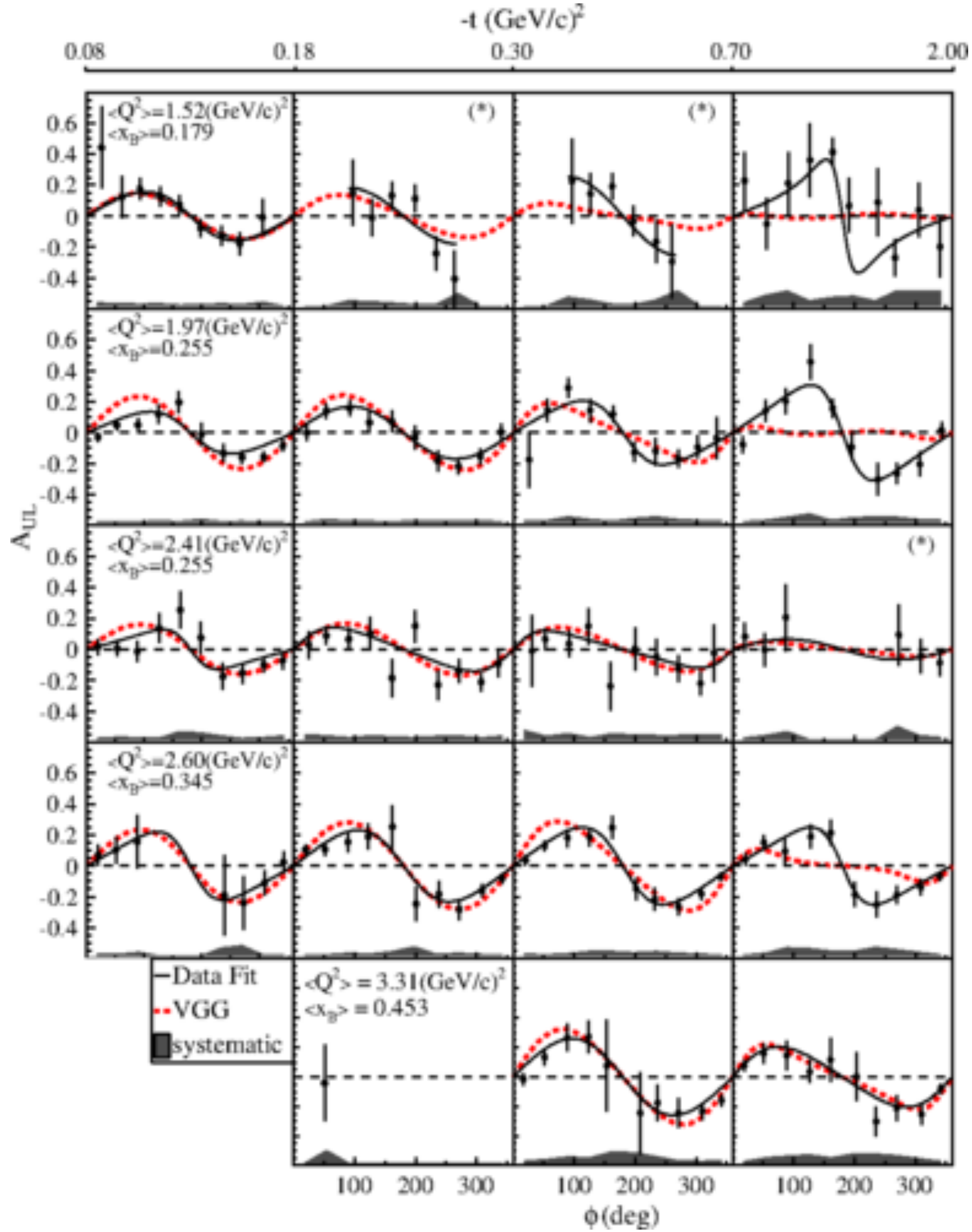

E. Seder *et al* (CLAS), ***PRL* 114** (2015) 032001

S. Pisano *et al* (CLAS), ***PRD* 91** (2015) 052014

Beam- and target-spin asymmetries

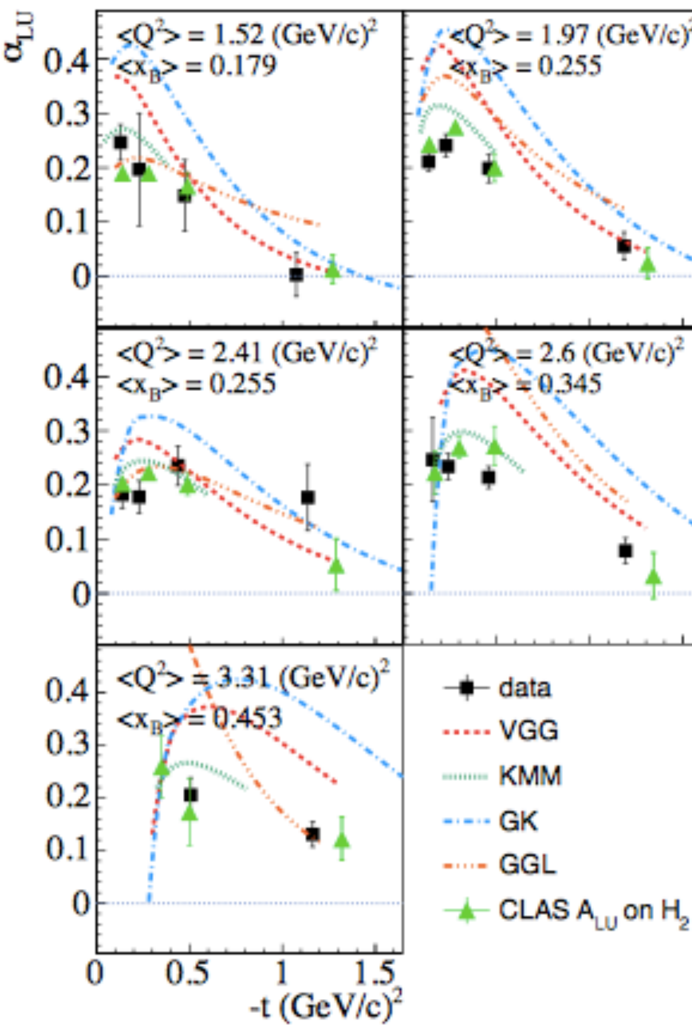

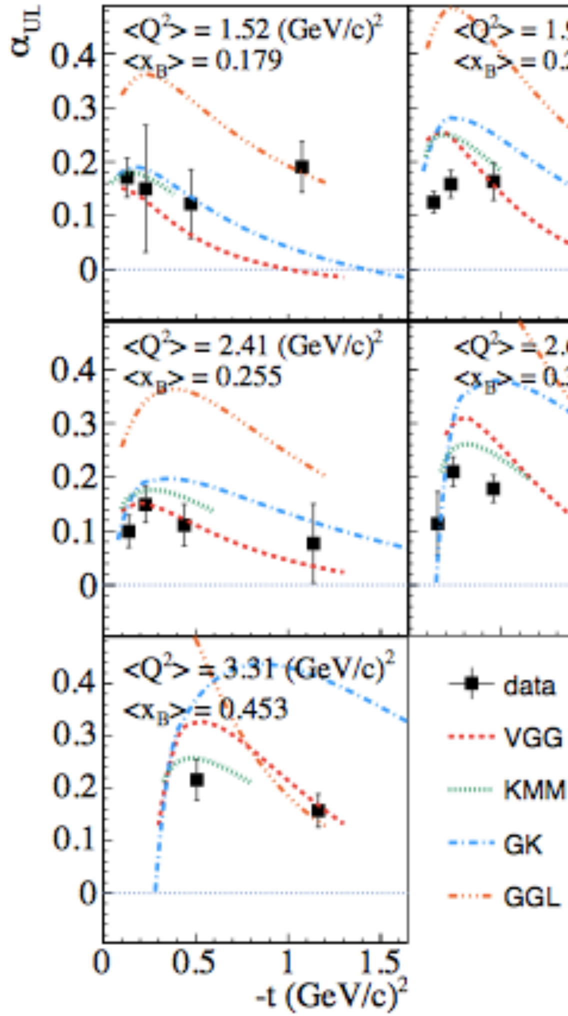

$$A = \frac{\alpha sin\phi}{1+\beta cos\phi}$$

GGL: Goldstein, Gonzalez, Liuti

GK: Kroll, Moutarde, Sabatié

KMM: Kumericki, Mueller, Murray

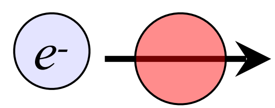

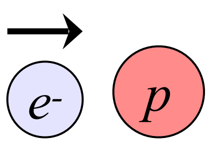

S. Pisano *et al* (CLAS), ***PRD* 91** (2015) 052014
E. Seder *et al* (CLAS), ***PRL* 114** (2015) 032001

* TSA shows a flatter distribution in *t* than BSA.

Double-spin asymmetry

At leading twist, double-spin asymmetry (DSA) can be expressed as:

$$A_{\mathrm{LL}}(\phi) \sim \frac{c^{\mathrm{BH}}_{0,\mathrm{LP}} + c^{\mathcal{I}}_{0,\mathrm{LP}} + (c^{\mathrm{BH}}_{1,\mathrm{LP}} + c^{\mathcal{I}}_{1,\mathrm{LP}}) \cos\phi}{c^{\mathrm{BH}}_{0,\mathrm{unp}} + (c^{\mathrm{BH}}_{1,\mathrm{unp}} + c^{\mathcal{I}}_{1,\mathrm{unp}} + \ldots) \cos\phi \ldots}$$

$$c^{\mathcal{I}}_{0,\mathrm{LP}}, c^{\mathcal{I}}_{1,\mathrm{LP}} \propto \Re\mathrm{e}[F_1 \widetilde{\mathcal{H}} + \xi(F_1 + F_2)(\mathcal{H} + \frac{x_B}{2}\mathcal{E}) - \xi(\frac{x_B}{2}F_1 + \frac{t}{4M^2}F_2)\widetilde{\mathcal{E}}]$$

At CLAS kinematics, leading-twist dominance of these CFFs

* Fit function for the phi-dependence of the asymmetry: $\dfrac{\kappa_{\mathrm{LL}} + \lambda_{\mathrm{LL}} \cos\phi}{1 + \beta\cos\phi}$

Shares denominator with BSA and TSA!
If measurements at same kinematics, can do a simultaneous fit.

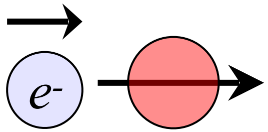

Double-spin Asymmetry (A_{LL})

CLAS

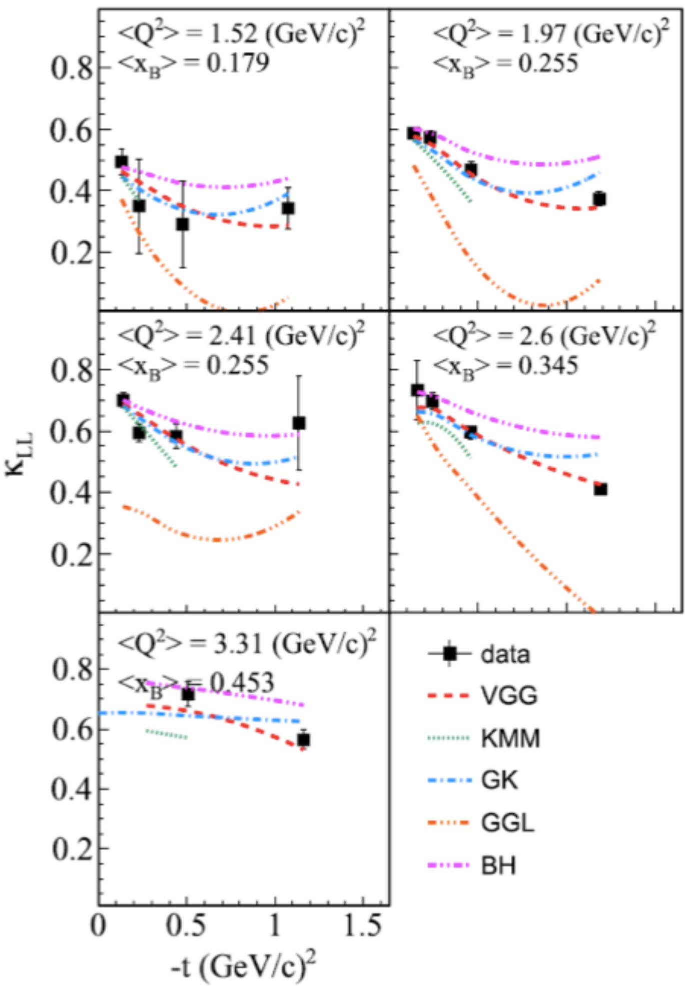

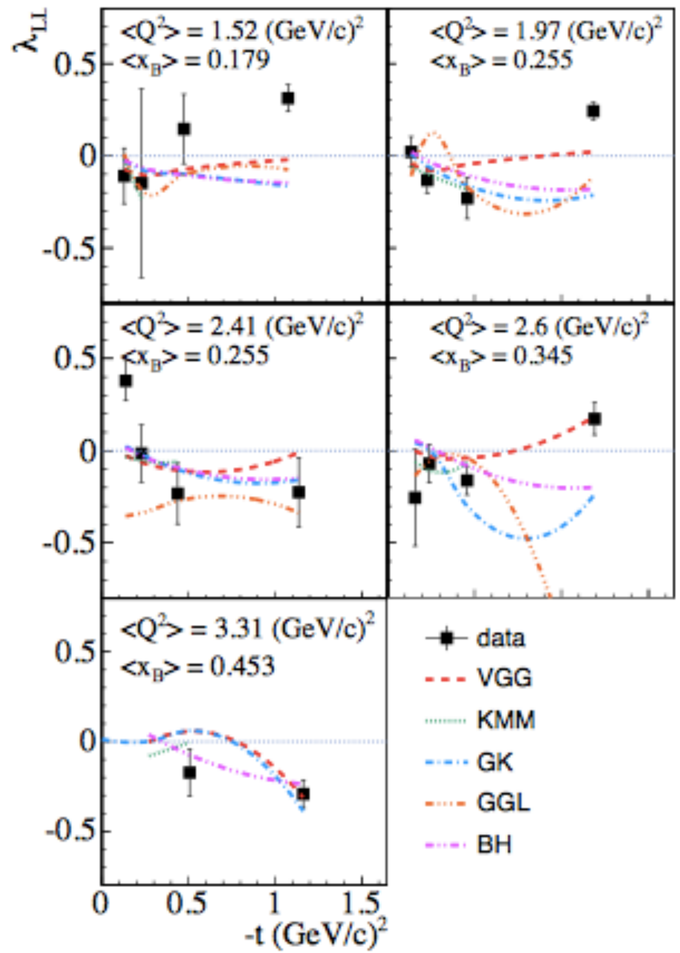

A_{LL} from fit to asymmetry:

$$\frac{\kappa_{LL} + \lambda_{LL}\cos\phi}{1 + \beta\cos\phi}$$

A_{LL} characterised by real parts of CFFs via:

$$F_1 \tilde{H} + \xi G_M \left(H + \frac{x_B}{2} E\right) + \ldots$$

- Fit parameters extracted from a simultaneous fit to BSA, TSA and DSA.
- Constant term dominates and is almost entirely BH.

E. Seder *et al* (CLAS), ***PRL* 114** (2015) 032001

S. Pisano *et al* (CLAS), ***PRD* 91** (2015) 052014

CFF extraction from three spin asymmetries at common kinematics.

What can we learn from the asymmetries?

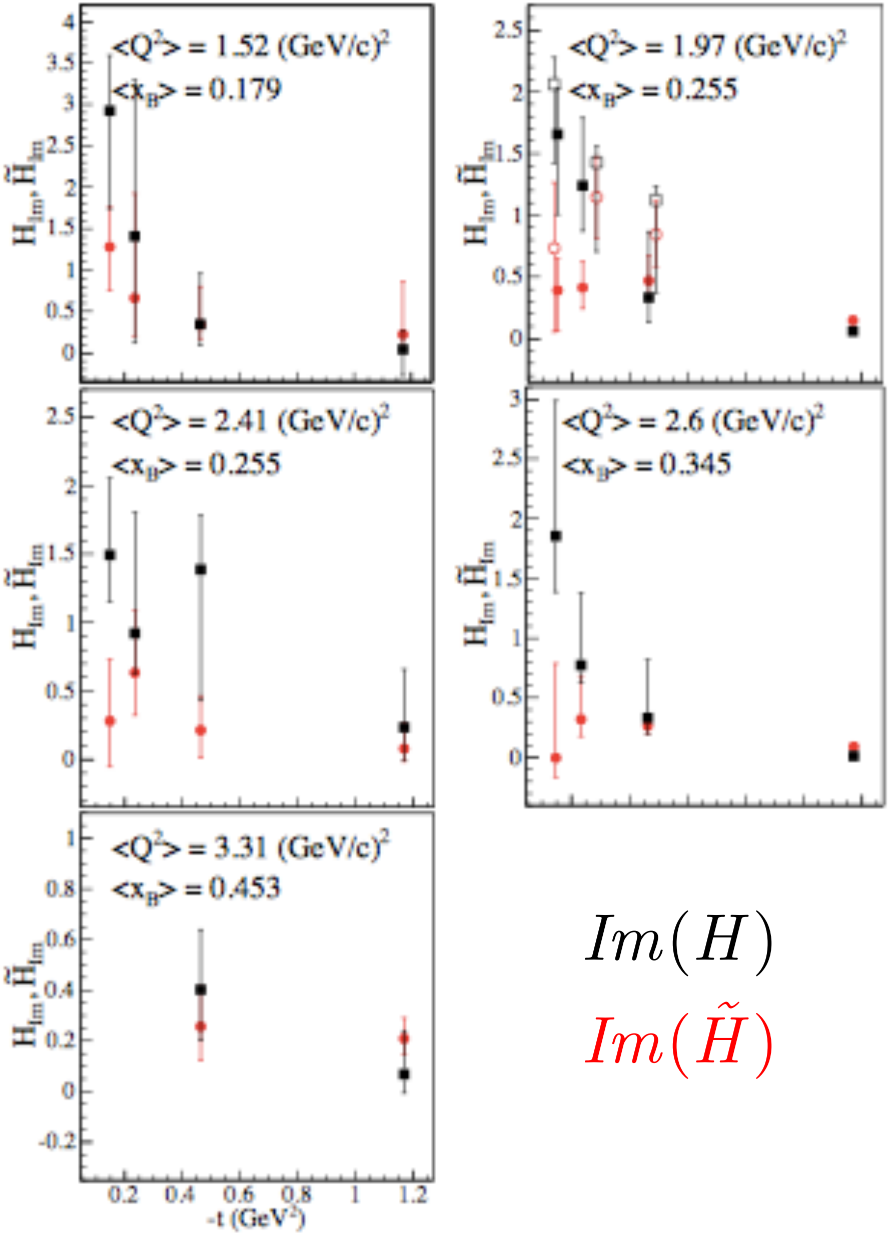

$Im(H)$

$Im(\tilde{H})$

Answers hinge on a global analysis of all available data.

- Information on relative distributions of quark momenta (PDFs) and quark helicity, $\Delta q(x)$.

$$H(x,0,0) = q(x) \quad \tilde{H}(x,0,0) = \Delta q(x)$$

- Indications that axial charge is more concentrated than electromagnetic charge.

$$\int_{-1}^{+1} H dx = F_1$$

$$\int_{-1}^{+1} \tilde{H}\, dx = G_A$$

E. Seder *et al* (CLAS), ***PRL*** **114** (2015) 032001
S. Pisano *et al* (CLAS), ***PRD*** **91** (2015) 052014

DVCS cross-sections @ CLAS

- Three months in 2005
- 5.79 GeV polarised electron beam (79.4% polarisation)
- 2.5cm long liquid H_2 target

- CLAS + IC detectors
- Luminosity = 2 x 10^{34} $cm^{-2}s^{-1}$
- Exclusive reconstruction:

$$ep \to e'p'\gamma$$

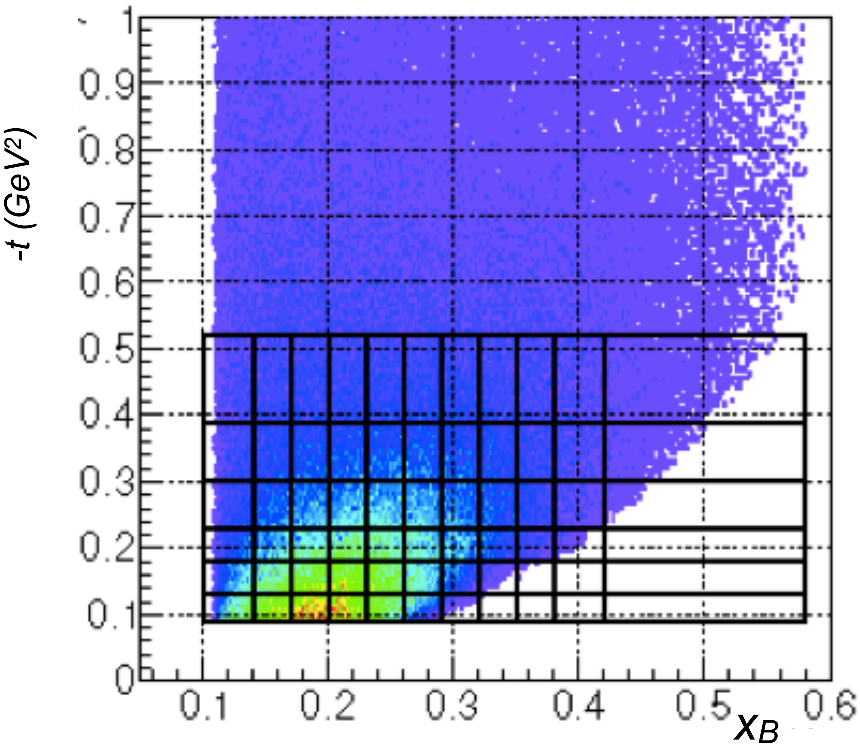

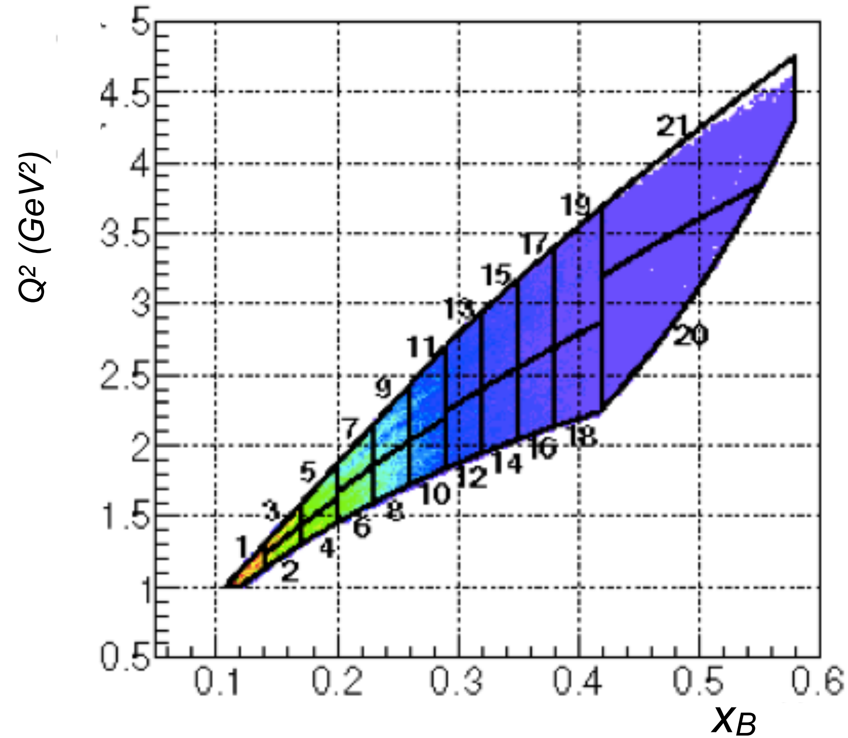

H.-S. Jo *et al* (CLAS), ***PRL*** **115** (2015) 212003

DVCS cross-sections @ CLAS

- Widest phase space coverage in valence quark region: CFF constraints.
- Dominance of GPD H in unpolarised cross-section.

$$\frac{d^4\sigma_{ep\to ep\gamma}}{dQ^2 dx_B dt d\Phi}$$

$$\frac{1}{2}\left(\frac{d^4\overrightarrow{\sigma}_{ep\to ep\gamma}}{dQ^2 dx_B dt d\Phi} - \frac{d^4\overleftarrow{\sigma}_{ep\to ep\gamma}}{dQ^2 dx_B dt d\Phi}\right)$$

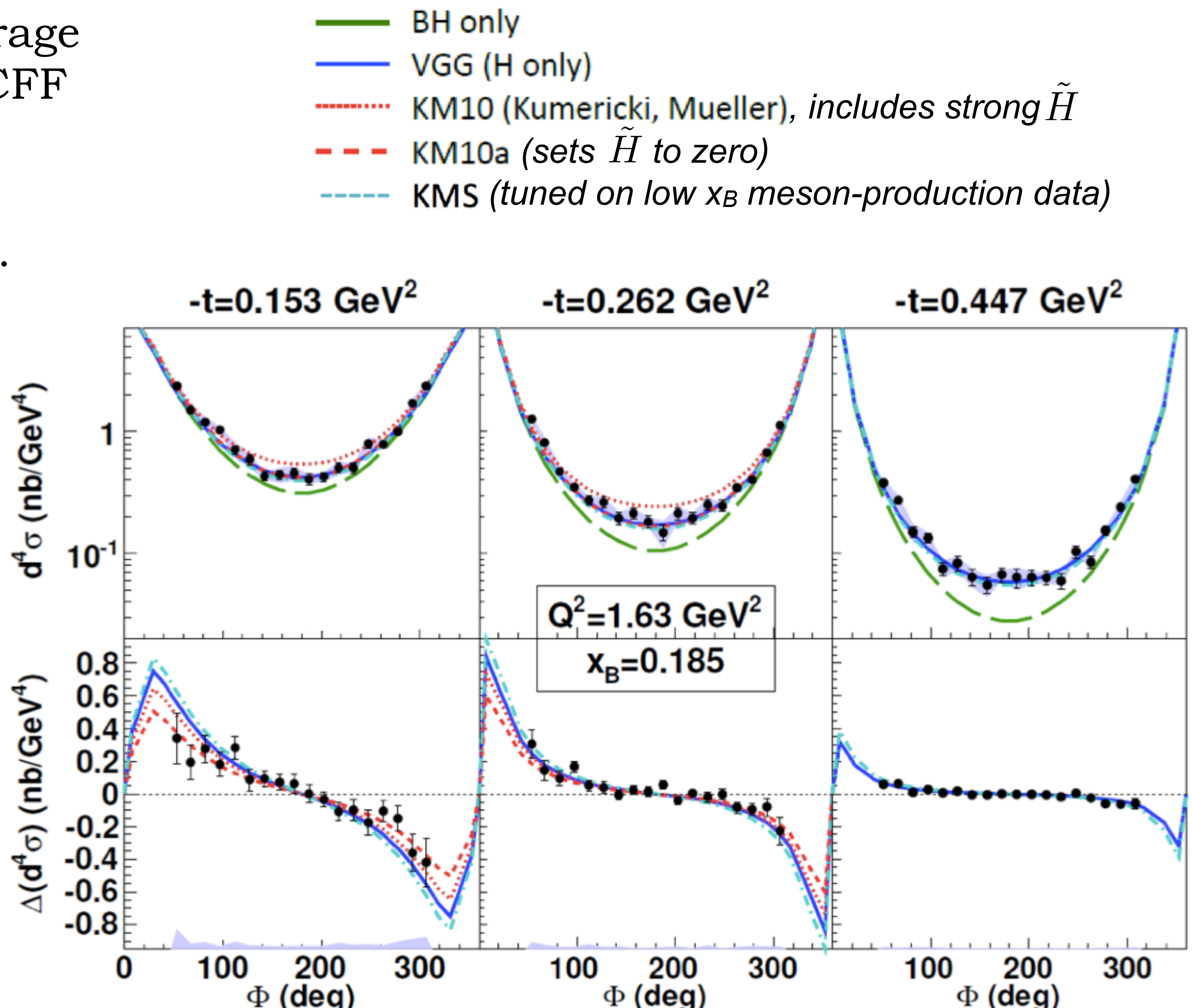

H.-S. Jo *et al* (CLAS), ***PRL* 115** (2015) 212003

Towards nucleon tomography

CLAS

- CFFs extracted in a VGG fit.
- Imaginary part of CFF: $F_{Im}(\xi, t) = F(\xi, \xi, t) \mp F(-\xi, \xi, t)$

VGG prediction

Ae^{bt}

- H_{Im} slope in t becomes flatter at higher x_B

Valence quarks at centre, sea quarks spread out towards the periphery.

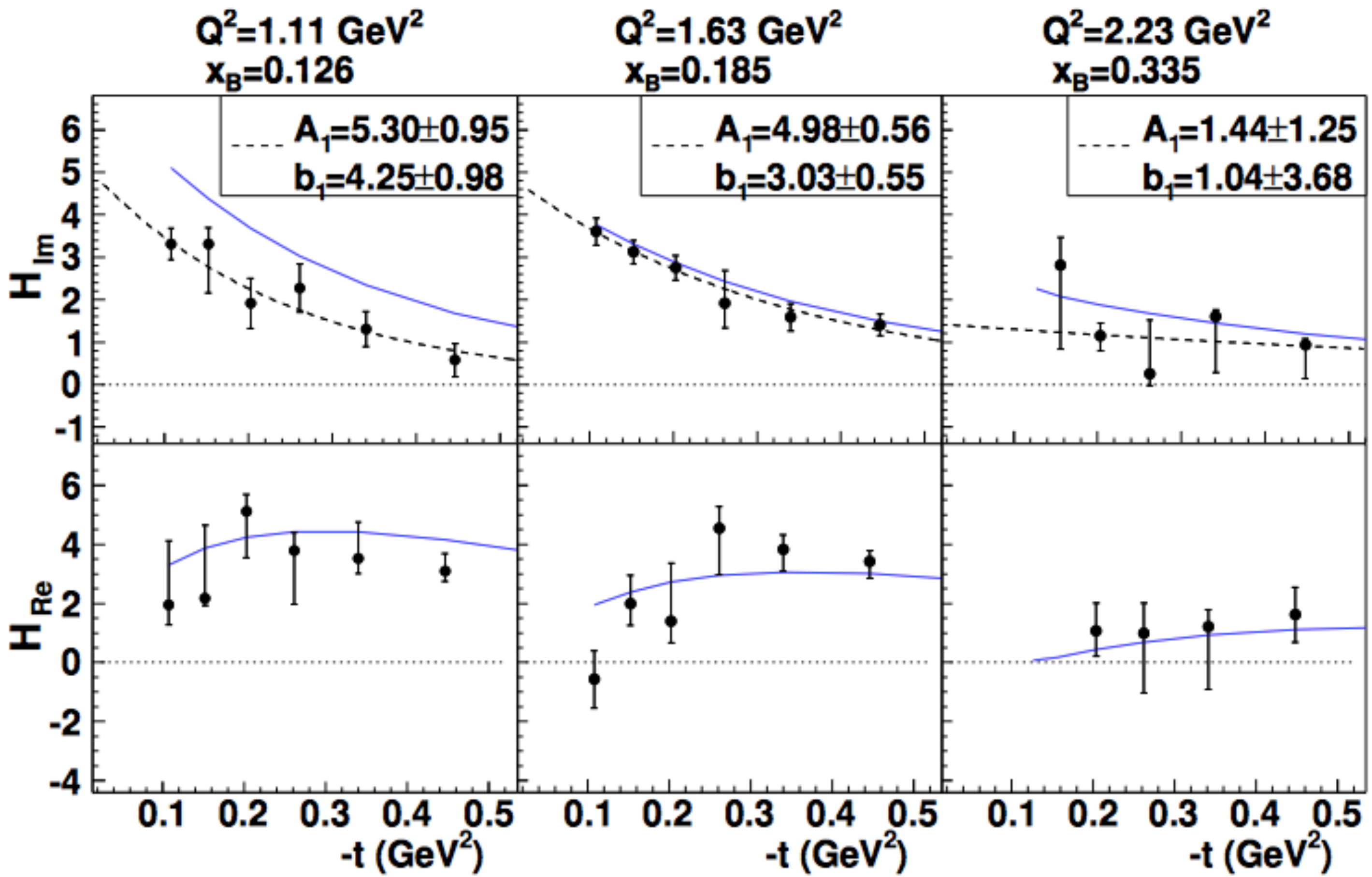

H.-S. Jo *et al* (CLAS Collaboration), ***PRL*** **115** (2015) 212003

Towards nucleon tomography

Quasi model-independent extraction of CFFs based on a local fit:

- Set 8 CFFs as free parameters to fit, at each (x_B,t) point, the available observables.
- Limits imposed within +/- 5 times the VGG model predictions (Vanderhaeghen-Guichon-Guidal).
- Relies on knowledge of BH and leading-twist DVCS amplitude parametrisation.

The best constraints in fits to CLAS data were obtained on H_{IM}.

Parametrise its dependence on t:

$$H_{Im}(\xi, t) = A(\xi)e^{B(\xi)t}$$

Relates to quark density

Inverse relation to spatial distribution

In principle, can obtain quark distributions at different x, but only have access to the points $x = \xi$ and the interpretation only applies at $\xi = 0$.

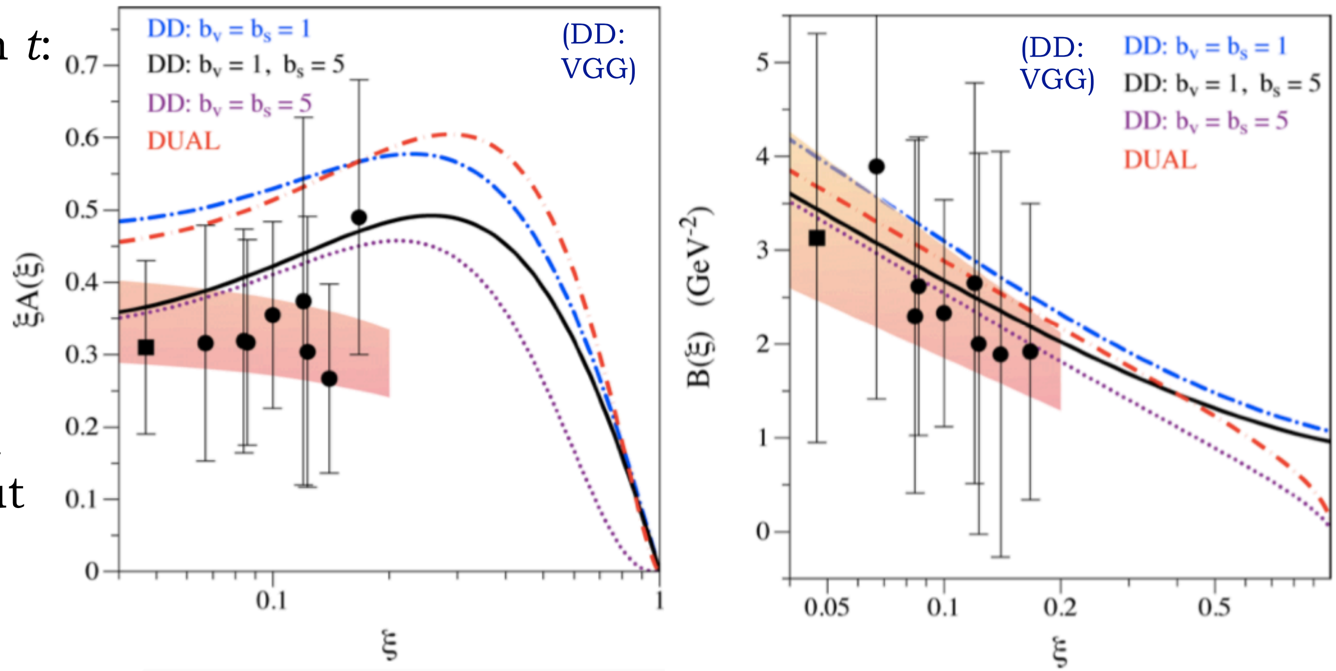

R. Dupré *et al.*, arXiv:1704.07330 [hep-ph]

Towards nucleon tomography

Further, can relate the impact parameter to helicity-averaged transverse charge distribution:

$$\rho^q(x, \mathbf{b}_\perp) = \int \frac{d^2\mathbf{\Delta}_\perp}{(2\pi)^2} e^{-i\mathbf{b}_\perp \cdot \mathbf{\Delta}_\perp} H^q_-(x, 0, -\mathbf{\Delta}_\perp{}^2)$$

Transverse four-momentum transfer to nucleon

$$H^q_-(x, 0, t) \equiv H^q(x, 0, t) + H^q(-x, 0, t)$$

Assuming leading-twist and exponential dependence of GPD on t, using models to extrapolate to the zero skewness point $\xi = 0$ and assuming similar behaviour for u and d quarks there:

$$\langle b_\perp^2 \rangle^q(x) = -4 \frac{\partial}{\partial \mathbf{\Delta}_\perp^2} \ln H^q_-(x, 0, -\mathbf{\Delta}_\perp{}^2) \Big|_{\mathbf{\Delta}_\perp = 0}$$

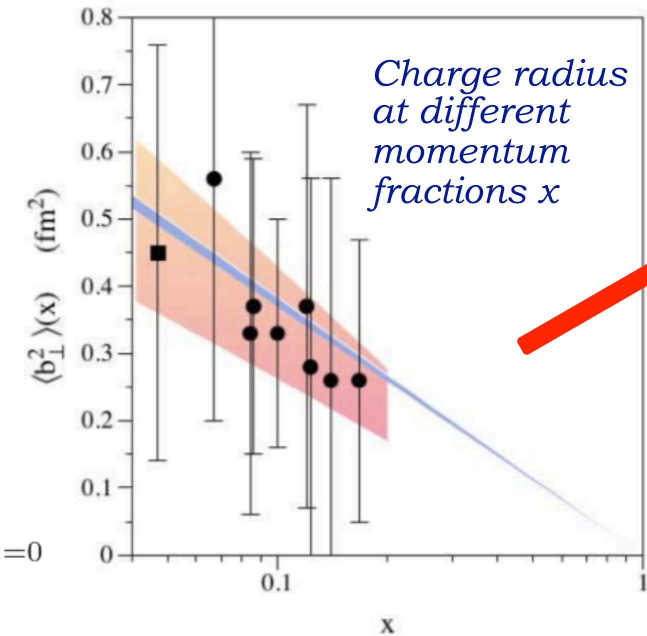

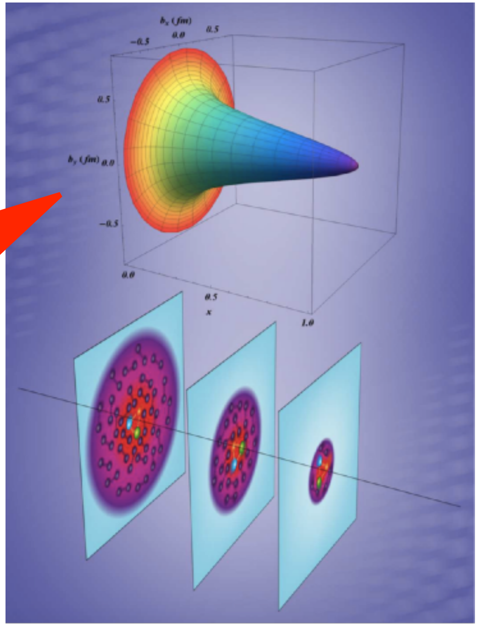

Not enough information yet for a conclusive picture, but tentative hints of 3D distributions are emerging!

R. Dupré *et al.*, arXiv:1704.07330 [hep-ph]

DVCS cross-sections in Hall A

* 15 cm long liquid H_2 target
* Luminosity $=10^{37}$ cm^{-2}s^{-1}

$$ep \rightarrow e'\gamma(p')$$

Detected in High Resolution Spectrometer (SRS)

Detected in PbF_2 Calorimeter

Reconstructed through missing mass

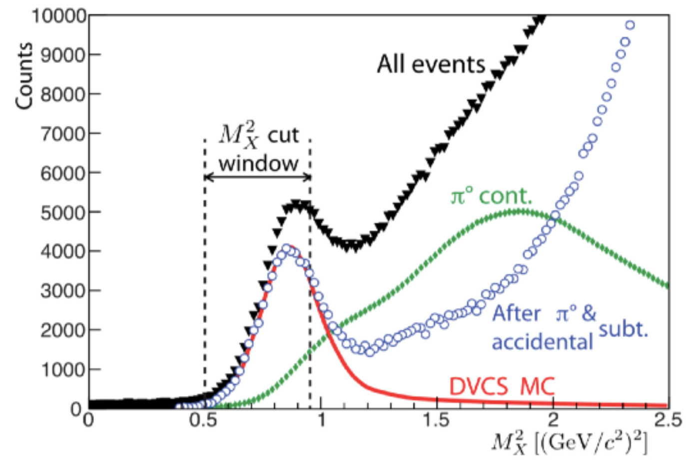

M. Defurne *et al*, ***PRC* 92** (2015) 055202.

* **E00-110 experiment** (2004):
5.75 GeV polarised electron beam

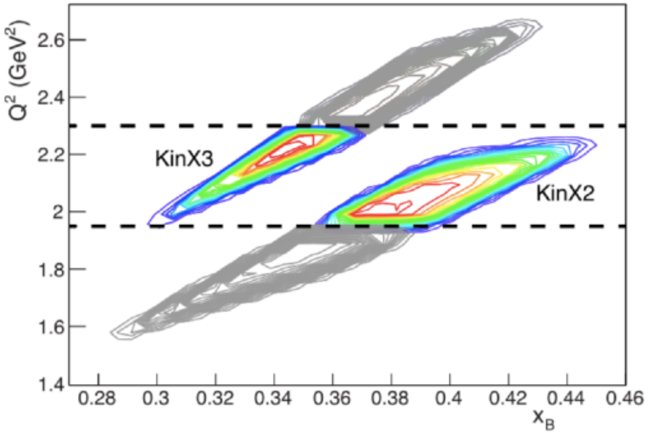

M. Defurne *et al*, ***PRC* 92** (2015) 055202.

* **E07-004 experiment** (2010):

Energy scan for fixed x_B, Q^2:

Q^2 (GeV^2)	x_B	E^{beam} (GeV)	$-t$ (GeV^2)
1.50	0.36	3.355 5.55	0.18, 0.24, 0.30
1.75	0.36	4.455 5.55	0.18, 0.24, 0.30, 0.36
2.00	0.36	4.455 5.55	0.18, 0.24, 0.30, 0.36

Can we assume leading twist?

- Twist: powers of $\frac{1}{\sqrt{Q^2}}$ in the DVCS amplitude. Leading-twist (LT) is twist-2.
- Order: introduces powers of α_s
- LO requires $Q^2 >> M^2$ (M: target mass)

  Bold assumption for JLab 6 GeV kinematics!

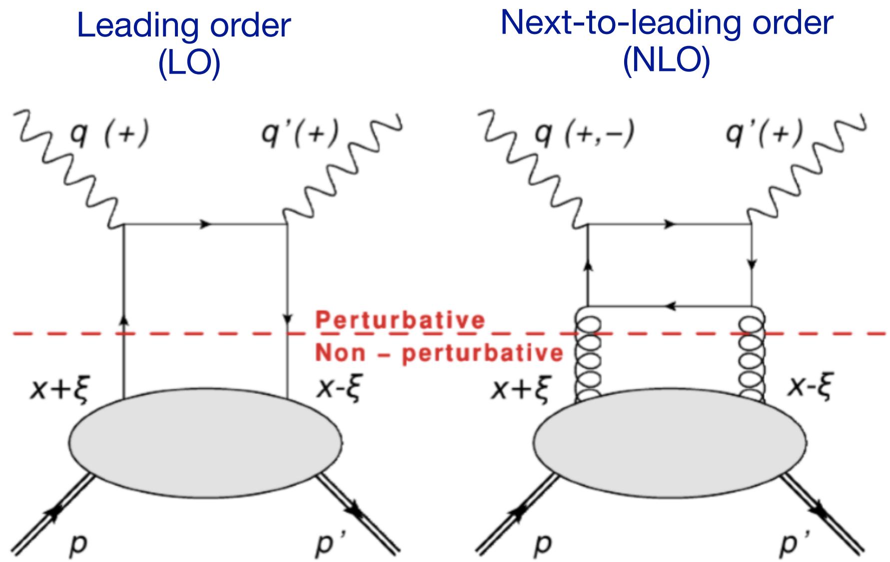

- CFFs can be classified according to real and virtual photon helicity:

$\mathcal{F}_{++}$

helicity of real produced photon

helicity of virtual incoming photon

  - Helicity-conserved CFFs — $\mathcal{F}_{++}$
  - Helicity-flip (transverse) — $\mathcal{F}_{-+}$
  - Longitudinal to transverse flip — $\mathcal{F}_{0+}$

- CFFs contributing to the scattering amplitude:
  - LT in LO: only $\mathcal{F}_{++}$
  - LT in NLO: both $\mathcal{F}_{++}$ and $\mathcal{F}_{-+}$
  - Twist-3: $\mathcal{F}_{0+}$

Can we assume leading twist?

- At finite Q^2 and non-zero t there's ambiguity in defining the light-cone axis for the GPDs:
  - Traditional GPD phenomenology uses the Belitsky convention, in plane of q and P:
    A. Belitsky *et al*, ***Nucl. Phys. B878*** (2014), 214
  - New, Braun definition using q and q': more natural.
    V. Braun *et al*, ***Phys. Rev. D89*** (2014), 074022

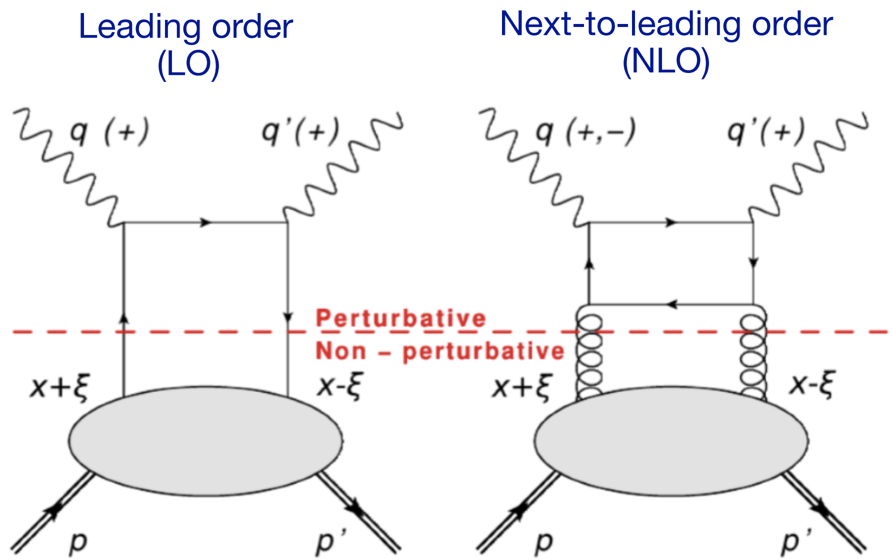

Reformulating CFFs in the Braun frame:

$$\mathcal{F}_{++} = \mathbb{F}_{++} + \frac{\chi}{2}\left[\mathbb{F}_{++} + \mathbb{F}_{-+}\right] - \chi_0 \mathbb{F}_{0+}$$
$$\mathcal{F}_{-+} = \mathbb{F}_{-+} + \frac{\chi}{2}\left[\mathbb{F}_{++} + \mathbb{F}_{-+}\right] - \chi_0 \mathbb{F}_{0+}$$
$$\mathcal{F}_{0+} = -(1+\chi)\mathbb{F}_{0+} + \chi_0\left[\mathbb{F}_{++} + \mathbb{F}_{-+}\right]$$

Belitsky CFFs

Braun CFFs

Assuming LO and LT in the Braun frame leaves higher-twist, higher-order contributions in the Belitsky frame, scaled by kinematic factors χ and χ_0.

Non-negligible at the Q^2 and x_B of the Hall A cross-section measurements in JLab @ 6 GeV era!

M. Defurne *et al*, ***Nature Communications 8*** (2017) 1408.

Hints of higher twist or higher orders

Hall A

- Strong deviation of the measured cross-section from Bethe-Heitler: a beam-energy scan can be used to identify pure DVCS and interference terms in a Rosenbluth-like separation, and to look for higher-twist effects.

→ E07-007: Hall A experiment to measure helicity-dependent and -independent cross-sections at two beam energies and constant x_B and t.

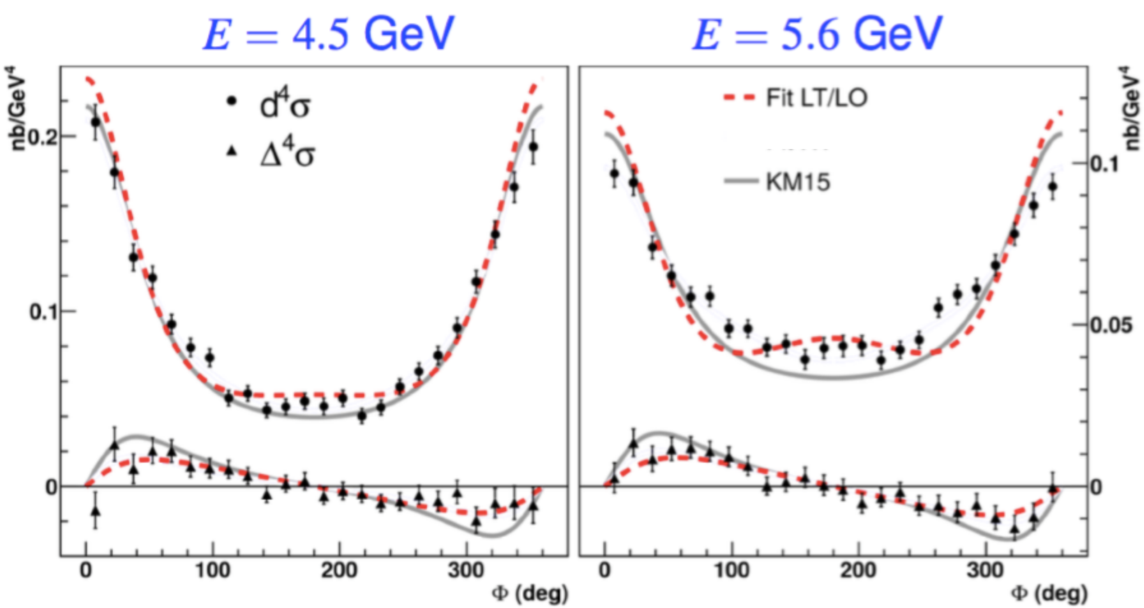

- Simultaneous fit to cross-sections at both energies and three values of Q^2 using only leading twist and leading order (LT/LO) do not describe the cross-sections fully: **higher twist/order effects?**

Using Braun's decomposition, $\mathbb{H}_{-+}$ and $\mathbb{H}_{0+}$ can't be neglected.

M. Defurne *et al*, ***Nature Communications* 8** (2017) 1408.

Hints of higher twist or higher orders

Hall A

* Including either higher order or higher twist effects (HT) improves the match with data:

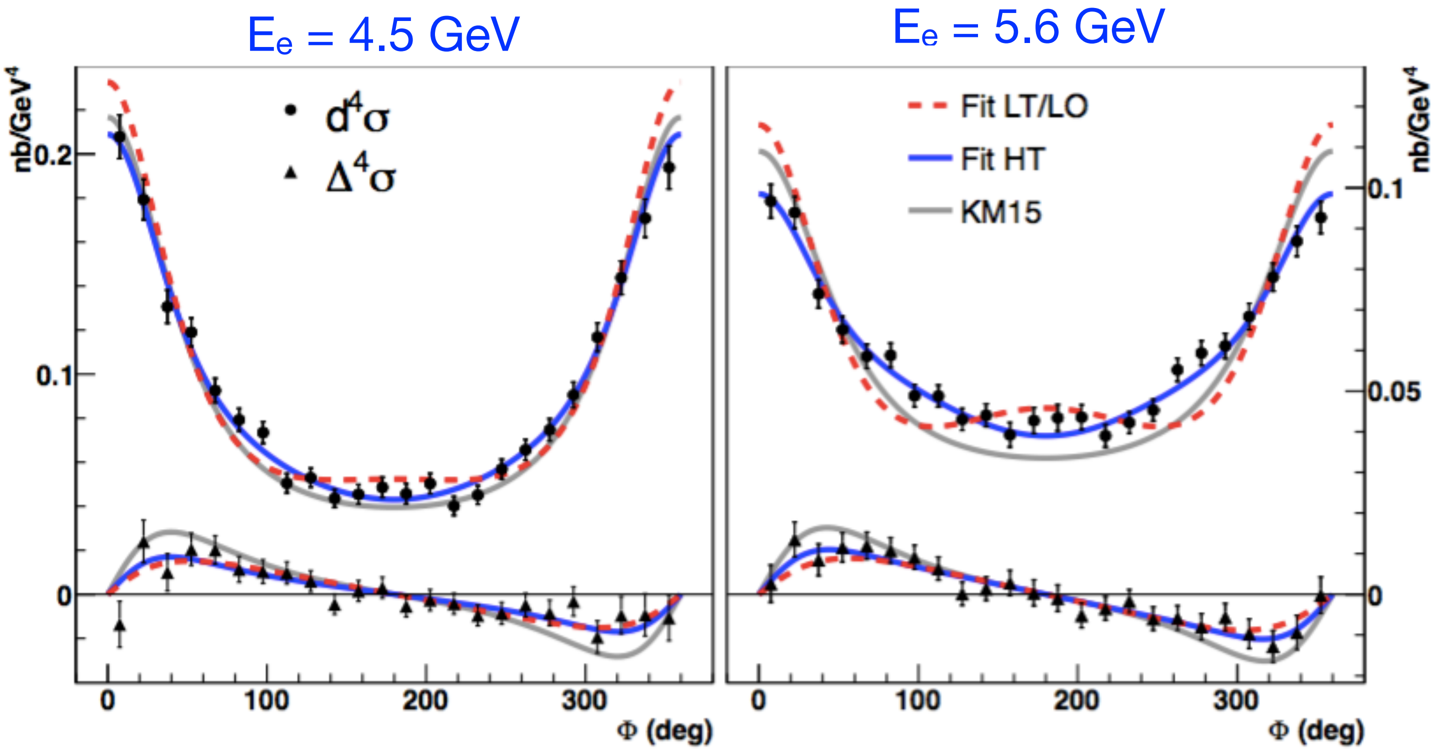

Higher-order and / or higher-twist terms are important! A glimpse of gluons.

Wider range of beam energy needed to identify the dominant effect → **JLab at 11 GeV.**

M. Defurne *et al*, ***Nature Communications* 8** (2017) 1408.

Rosenbluth separation of DVCS² and BH-DVCS terms

Hall A

- Generalised Rosenbluth separation of the DVCS² and the BH-DVCS interference terms in the cross-section is possible but NLO and/or higher-twist required.

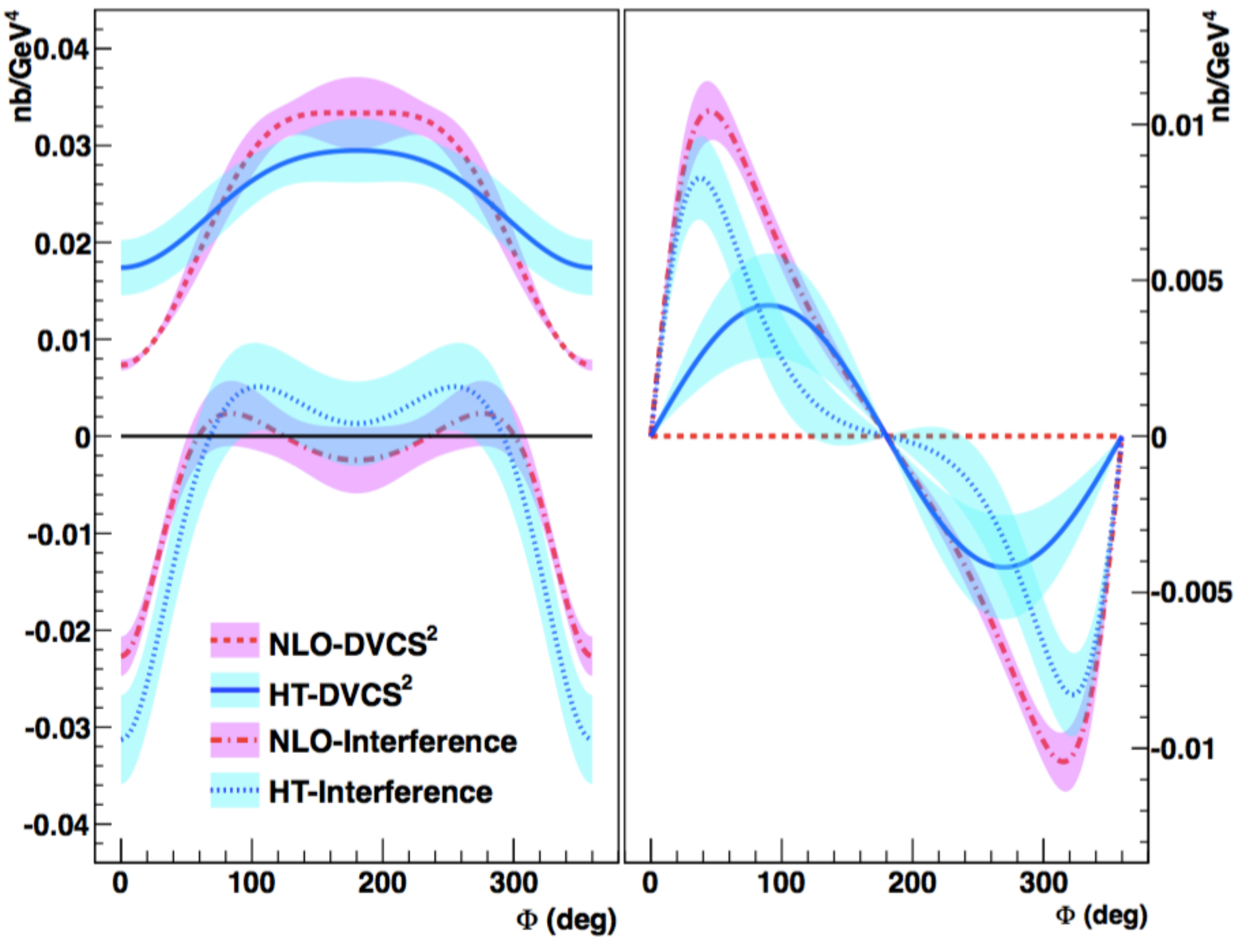

- Significant differences between pure DVCS and interference contributions.
- Helicity-dependent cross-section has a sizeable DVCS² contribution in the higher-twist scenario.
- Separation of HT and NLO effects requires scans across wider ranges of Q^2 and beam energy: JLab12!

M. Defurne *et al*, ***Nature Communications 8*** (2017) 1408.

JLab @ 12 GeV

Hall A

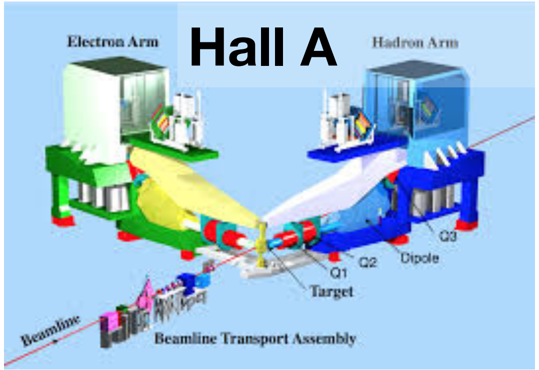

High resolution($\delta p/p = 10^{-4}$) spectrometers, very high luminosity, large installation experiments.

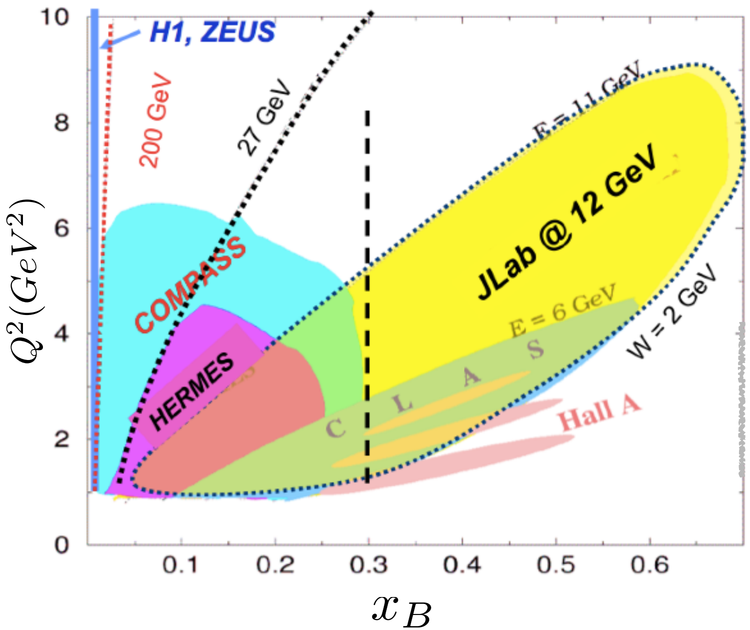

Hall C

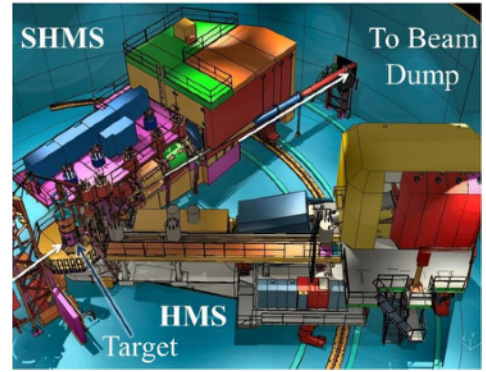

Two movable high momentum spectrometers, well-defined acceptance, very high luminosity.

Hall D

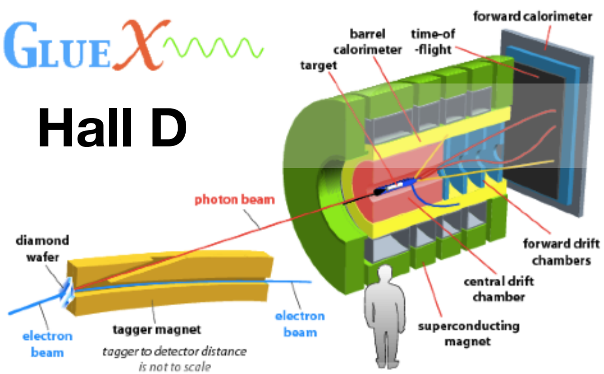

9 GeV tagged polarised photons, full acceptance

Hall B: CLAS12

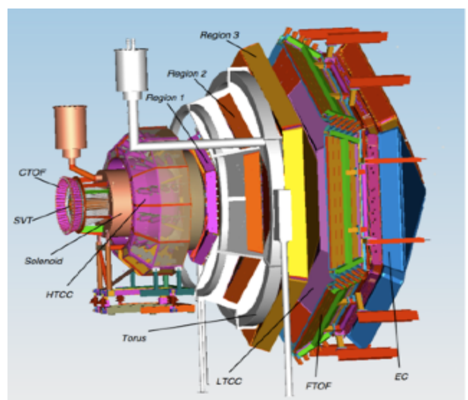

Very large acceptance, high luminosity.

CLAS12

Design luminosity

$L \sim 10^{35}\ \mathrm{cm}^{-2}\ \mathrm{s}^{-1}$

High luminosity & large acceptance:
Concurrent measurement of exclusive, semi-inclusive, and inclusive processes

Acceptance for photons and electrons:
- $2.5^{\circ} < \theta < 125^{\circ}$

Acceptance for all charged particles:
- $5^{\circ} < \theta < 125^{\circ}$

Acceptance for neutrons:
- $5^{\circ} < \theta < 120^{\circ}$

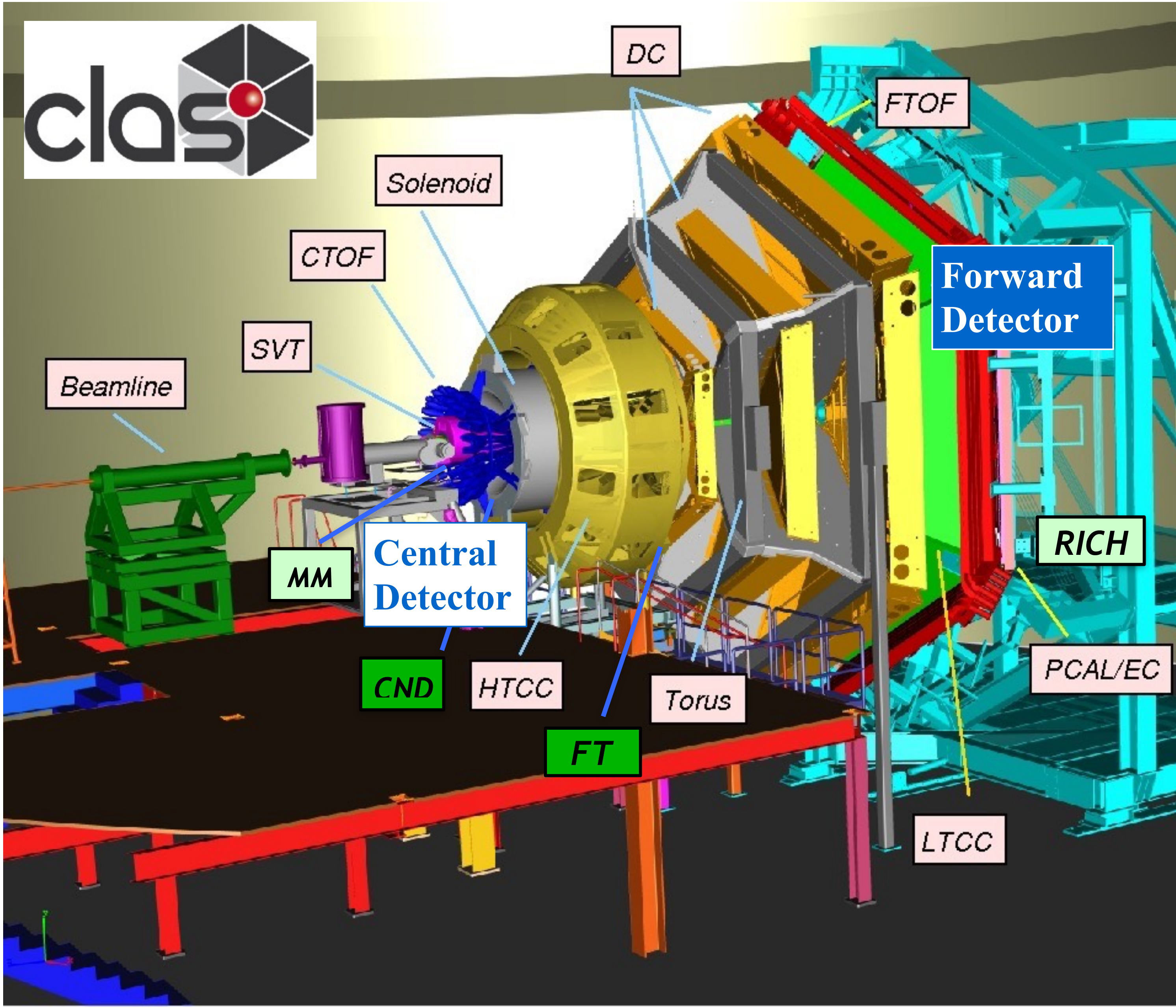

CLAS12 assembled

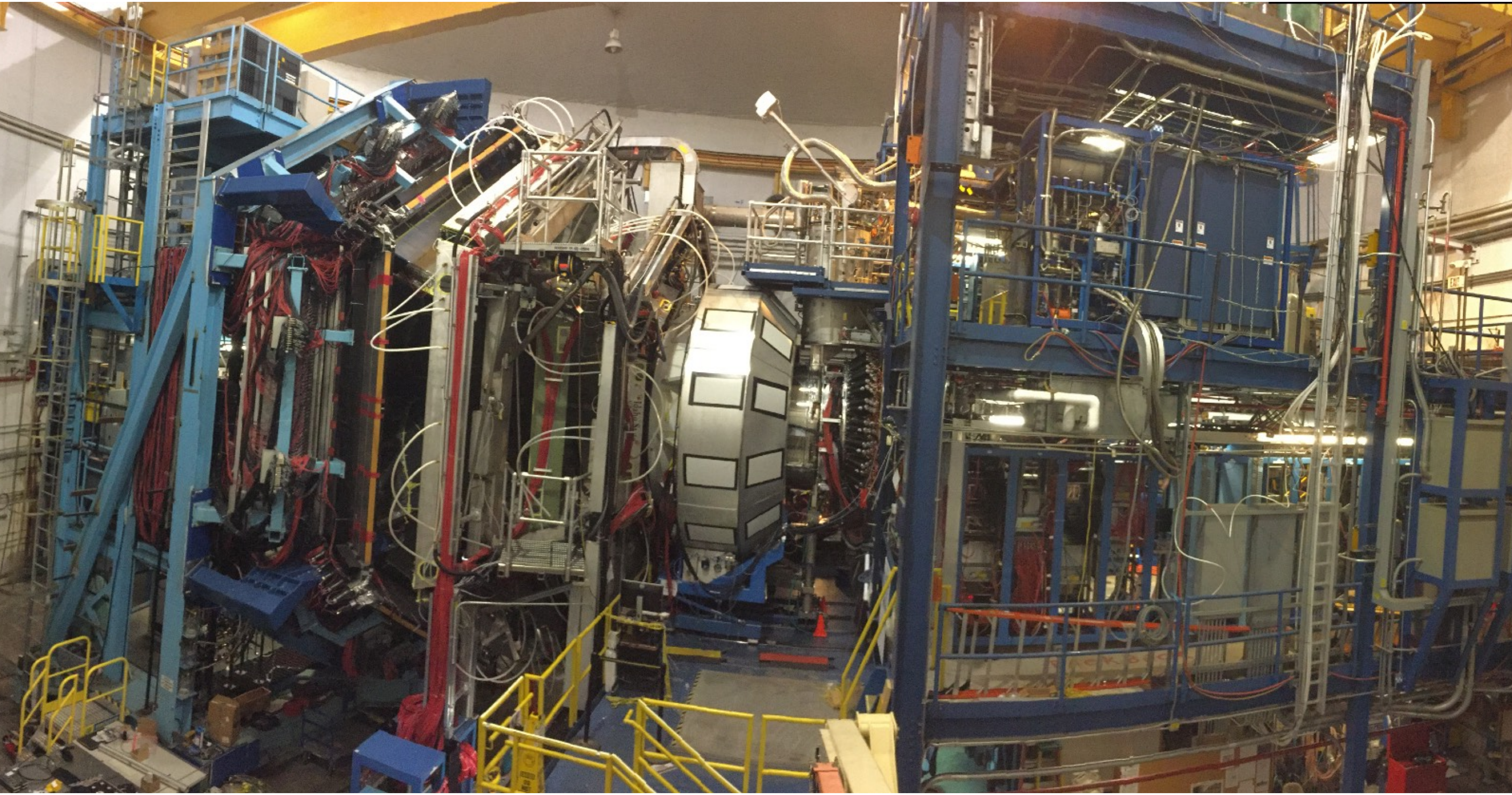

DVCS in CLAS12: detection

* **Electrons** detected and identified in the Forward Detector using similar techniques to CLAS: signal in Cerenkov detector, energy deposit in calorimeters and tracking through drift chambers in a toroidal magnetic field.

* **Protons**: tracking in a magnetic field, time of flight from scintillator paddles.

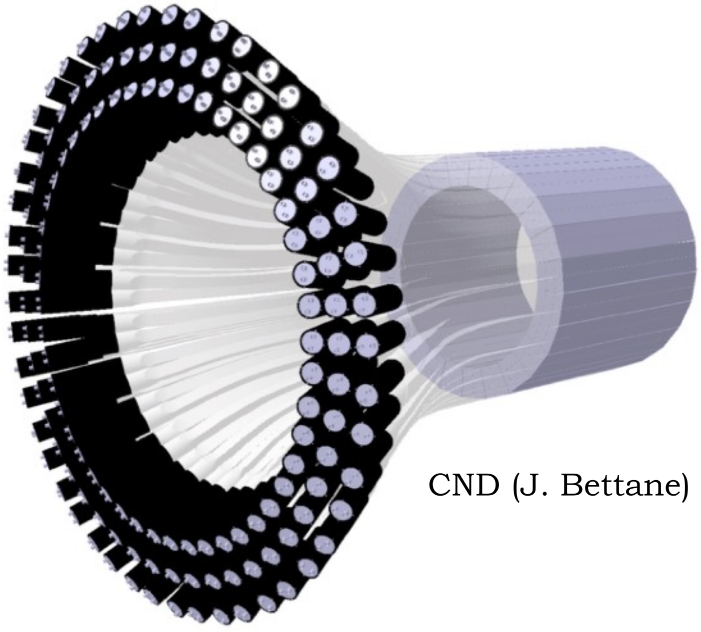

CND (J. Bettane)

* **Neutrons** in the Central Detector: on the basis of time of flight and energy deposit in the Central Neutron Detector scintillator barrel.

DVCS in CLAS12: detection

- **Photons** in the Forward Detector: energy deposit in the Calorimeters — EC and the Forward Tagger.

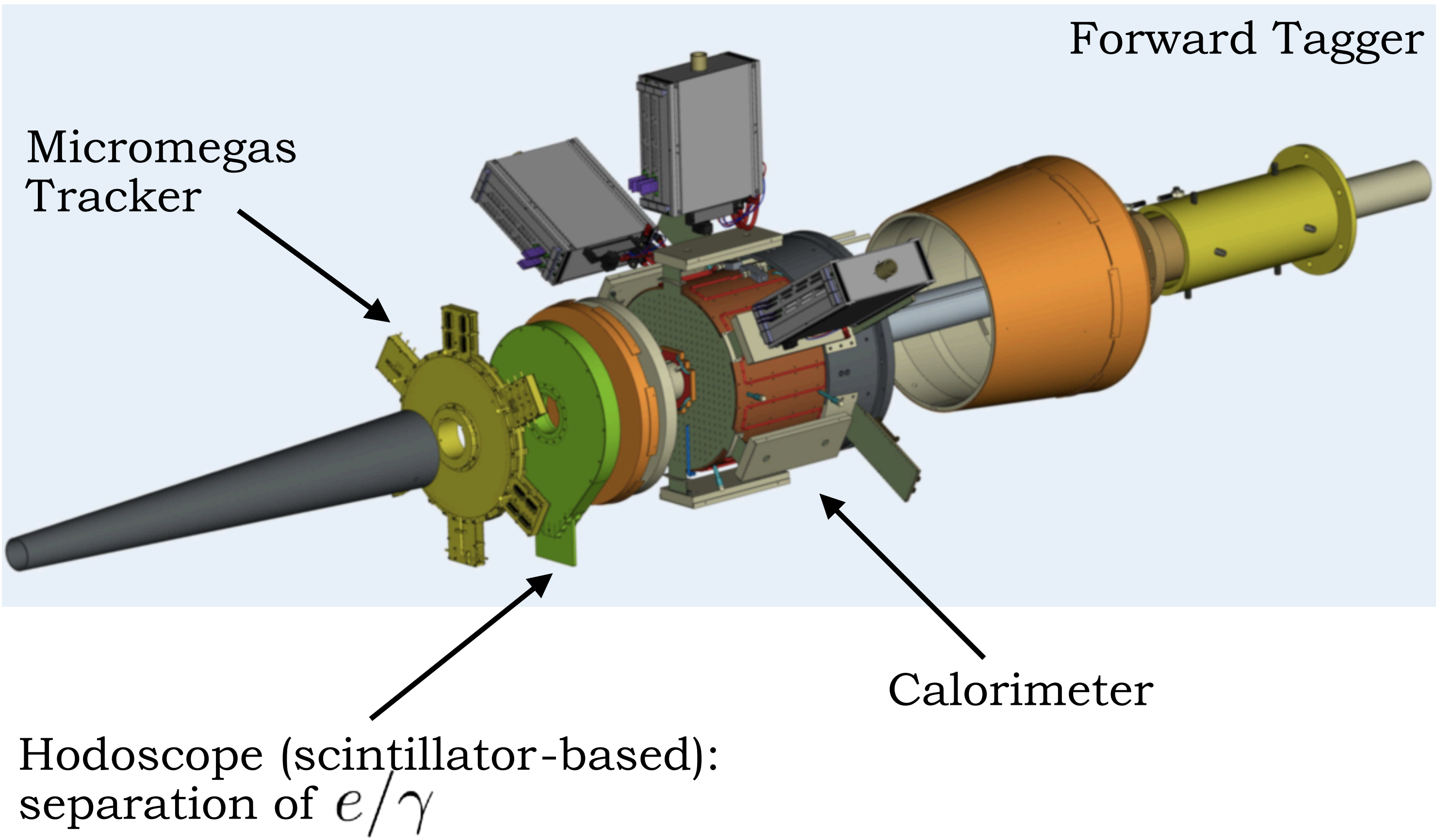

DVCS in Hall A @ 11 GeV

Detect electron in the Left High Resolution Spectrometer (HRS-L): 0.01% momentum resolution

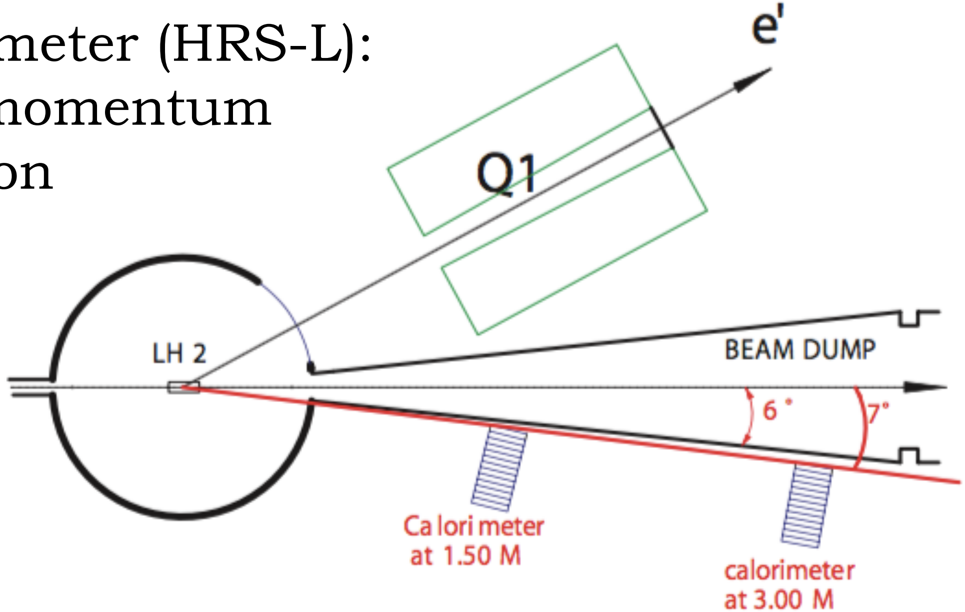

Detect photon in PbF_2 calorimeter: < 3% energy resolution

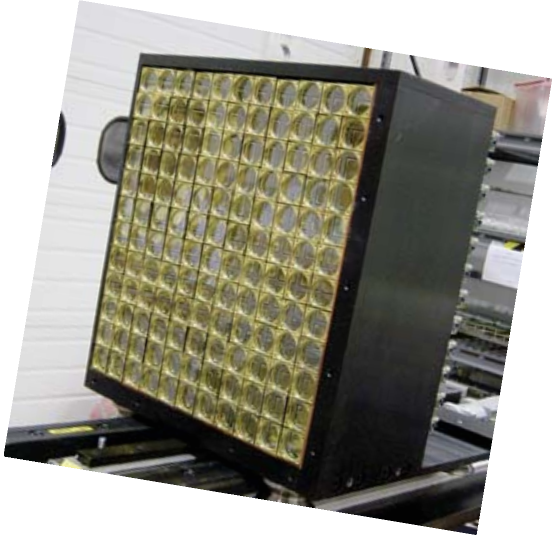

Reconstruct recoiling proton through missing mass.

DVCS in Hall C @ 11 GeV

Detect electron with (Super) High Momentum Spectrometer, (S)HMS.

Detect photon in $PbWO_4$ calorimeter.

Sweeping magnet to reduce backgrounds in calorimeter.

Reconstruct recoiling proton through missing mass.